

1
2
3
4
5
6 **A New Tropical Savanna PFT, Variable Root Growth and Fire Improve Cerrado**
7 **Vegetation Dynamics Simulations in a Dynamic Global Vegetation Model**
8

9 Jéssica Schüler^{1,2*}, Sarah Bereswill^{2*}, Werner von Bloh²,
10 Maik Billing², Boris Sakschewski², Luke Oberhagemann^{2,3}, Kirsten Thonicke² and
11 Mercedes M.C. Bustamante¹

12
13 ¹ Department of Ecology, University of Brasília, Campus Universitário Darcy Ribeiro,
14 70910-900, Brasília, Brazil

15 ² Potsdam Institute for Climate Impact Research, Telegrafenberg A 31, 14473 Potsdam,
16 Germany

17 ³ Institute of Environmental Science and Geography, University of Potsdam, Karl-
18 Liebknecht Str. 24/25, Potsdam, Germany

19
20 *Correspondence to:* Jéssica Schüler (jehschuler@gmail.com)

21 **Abstract**

22 The Cerrado, South America's second largest biome, has been historically
23 underrepresented in Dynamic Global Vegetation Models (DGVMs). Therefore, this study
24 introduces a novel Plant Functional Type (PFT) tailored to the Cerrado biome into the
25 DGVM LPJmL-VR-SPITFIRE. The parametrization of the new PFT, called a Tropical
26 Broadleaved Savanna tree (TrBS), integrates key ecological traits of Cerrado trees,
27 including specific allometric relationships, wood density, specific leaf area (SLA), deep-
28 rooting strategies, and fire-adaptive characteristics. The inclusion of TrBS in LPJmL-VR-
29 SPITFIRE led to notable improvements in simulated vegetation distribution. TrBS became
30 dominant across Brazil's savanna regions, particularly in the Cerrado and Pantanal. The
31 model also better reproduced the above- and belowground biomass patterns, accurately
32 reflecting the "inverted forest" structure of the Cerrado, characterized by a substantial
33 investment in root systems. Moreover, the presence of TrBS improved the simulation of
34 fire dynamics, increasing estimates of burned area and yielding seasonal fire patterns more
35 consistent with observational data. Model validation confirmed the enhanced performance
36 of the model with the new PFT in capturing vegetation structure and fire regimes in Brazil.
37 Additionally, a global-scale test demonstrated reasonable alignment between the simulated
38 and observed global distribution of savannas. In summary, the integration of the TrBS PFT
39 marks a critical advancement for LPJmL-VR-SPITFIRE, offering a more robust
40 framework for investigating the interaction of above- with belowground ecological
41 processes, fire disturbance and the impacts of climate change across the Cerrado and other
42 tropical savanna ecosystems that together account for approximately 30 % of the primary
43 production of all terrestrial vegetation.

44

45 **1. Introduction**

46 Brazil spans over 850 million hectares, from approximately 5°N to 35°S, and hosts
47 diverse climatic conditions, from subtropical and semi-arid to tropical wet environments
48 (IBGE, 2024; Table S1). Within this context, the Cerrado is recognized as the world's most
49 biodiverse savanna and the second-largest vegetation formation in South America,
50 covering about 23% of Brazil (~2 million km²), mainly in the central region (Myers et al.,
51 2000; IBGE, 2024). The biome provides vital ecosystem services, including carbon
52 storage, climate regulation, and water resources for major river basins (Sano et al., 2019;
53 Schüller & Bustamante, 2022). Despite its global importance, the Cerrado faces severe
54 threats from deforestation driven by agricultural expansion and from climate change,
55 which is intensifying droughts and altering fire regimes, thereby accelerating biodiversity
56 loss and ecosystem degradation (Strassburg et al., 2017; Gomes et al., 2020a; Rodrigues
57 et al., 2022)..

58 Climate change impacts in Brazil are already evident. A study by INPE to the First
59 Biennial Transparency Report (MCTI, 2024) reveals an increase of approximately 20% in
60 the number of consecutive dry days in Brazil in recent decades, particularly in the North,
61 Northeast, and Central regions of the country. Similarly, Feron et al., (2024) demonstrated
62 an increase in the frequency of compound climate events involving heat, drought, and high
63 fire risk in key regions of South America, including the Amazon. A significant increase in
64 maximum and minimum temperatures was also observed in the Brazilian Cerrado between
65 1961 and 2019, along with a reduction in relative humidity (Hofmann et al., 2021).

66 In this context, vegetation modeling emerges as an essential tool for understanding and
67 predicting the Cerrado's responses to these pressures. Dynamic Global Vegetation Models
68 (DGVMs), such as the Lund-Potsdam-Jena managed Land model (LPJmL), aim to
69 simulate changes in vegetation, fire, water and carbon fluxes depending on climate and

70 land use (Cramer et al., 2001; Thonicke et al., 2010; Baudena et al., 2015; Moncrieff et al.,
71 2016; Schaphoff et al., 2018; Drüke et al., 2019; Martens et al., 2021). In order to reduce
72 complexity, common DGVMs classify vegetation into so-called Plant Functional Types
73 (PFTs), which are groups of plants that show similar responses to external drivers and
74 resemble their ecological function. PFTs are, in general, distinguished by their allometry,
75 growth form, phenology and photosynthetic strategy (Wullschleger et al., 2014).
76 Parameterization of PFTs should therefore capture the most important characteristics of
77 certain vegetation types while balancing complexity.

78 Specifically in savannas, vegetation is often characterized by small trees and shrubs that
79 grow deep roots and are well adapted to fire and drought, all of which distinguish them
80 from the trees in moist and seasonal tropical forests (Ratnam et al., 2011). However, many
81 DGVMs, including LPJmL, lack a dedicated savanna PFT, leading to significant
82 inconsistencies in model projections (Foley et al., 1998; Hughes, Valdes and Betts, 2006;
83 Clark et al., 2011; Neilson, R. P. 2015; Drüke; et al., 2019). This omission often results in
84 the underestimation of savanna vegetation extent and fire occurrences, while
85 overestimating above-ground biomass and the extent of tall tropical forest formations, as
86 demonstrated in simulations for South America (Cramer et al., 2001; Drüke et al., 2019),
87 or a depiction of savanna vegetation as tropical grasslands which do not encompass the
88 coexistence of grasses, shrubs and trees. DGVMs are, nevertheless, widely used to
89 simulate future transitions between the Amazon and the Cerrado biomes, often predicting
90 an abrupt shift from forest to grassland under climate change (Malhi et al., 2009; Swann
91 et al., 2015). However, this oversimplification neglects the intricate ecological gradient
92 that spans diverse vegetation types, from open forests to woody savannas with varying tree
93 cover densities.

94 This lack of precision in modeling has broader implications for understanding the
95 Cerrado's role in climate mitigation and adaptation, including nature restoration. For
96 example, restoring the entire 20 million hectares of the identified priority areas for
97 restoration in the Cerrado could remove up to 1.77 million tons of carbon from the
98 atmosphere (Schüler and Bustamante, 2022). Beyond carbon sequestration, savannas play
99 a crucial role in preserving water resources and biodiversity, acting as natural buffers
100 against climate change and enhancing ecosystem resilience (Oliver et al., 2015; Salazar et
101 al., 2016; Syktus and McAlpine 2016; Bustamante et al., 2019). With its highly seasonal
102 climate and diverse mosaic of grasslands, savannas, and forest formations, the Cerrado is
103 particularly significant for mitigating and adapting to climate change (Ribeiro and Walter
104 2008; Bustamante et al., 2019; Schüler and Bustamante 2022). Accurately representing
105 savanna-type vegetation in DGVMs will not only improve projections of the Cerrado's
106 vulnerability to climate change but also help identify high-risk areas and guide the
107 development of effective conservation, restoration, and management strategies. For
108 instance, improved models, acknowledging savanna-specific characteristics, could inform
109 studies investigating biome transitions and ecological tipping points, fire management
110 measures, support agricultural adaptation, and optimize water resource management,
111 ensuring the Cerrado's resilience in the face of environmental challenges.

112 We therefore introduce a new Cerrado specific PFT which we call “Tropical
113 Broadleaved Savanna tree” (TrBS) that entails the biome's unique characteristics into a
114 state-of-the-art version of the LPJmL model (LPJmL-VR-SPITFIRE). LPJmL-VR-
115 SPITFIRE explicitly simulates variable tree rooting strategies (Sakschewski et al., 2021)
116 and employs the process-based fire model SPITFIRE (Thonicke et al., 2010;
117 Oberhagemann et al., 2025), while being based on the latest LPJmL version (LPJmL 5.7;
118 Wirth et al., 2024). In this study, we test our new approach by modeling the Potential

119 Natural Vegetation (PNV) distribution for the entire Brazil and validate our results against
120 observational datasets. This model improvement provides a robust basis for studies
121 exploring the impact of climate change on vegetation dynamics in the Cerrado region. This
122 model is expected to show significant improvements in biomass estimate, vegetation type
123 distributions, and fire dynamics in tropical regions.

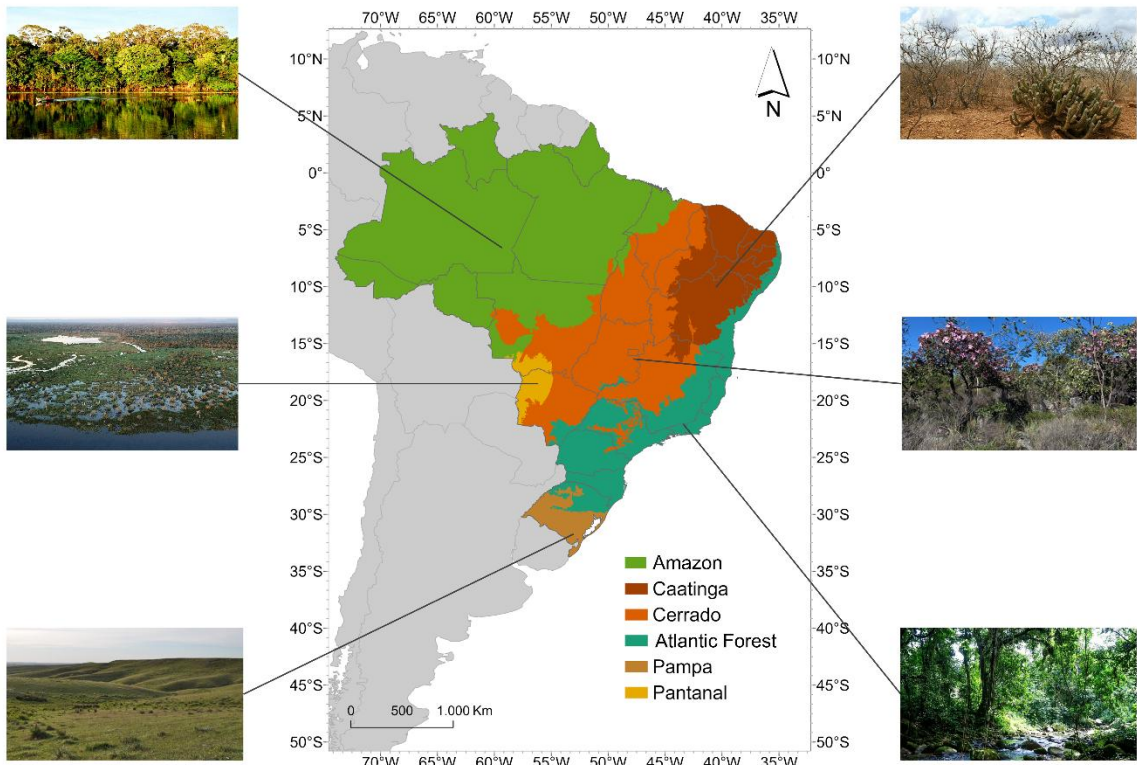
124 **2. Methods**

125 ***2.1 Study region***

126 Our study region encompasses all of the Brazilian territory, focusing on the distribution
127 of its six biomes, with special attention to the Cerrado biome. Because of its central
128 position, the Cerrado has ecotones with four of the other five Brazilian biomes: Amazon,
129 Caatinga, Atlantic Forest and Pantanal (Fig. 1).

130 Recognized as both a savanna and a global biodiversity hotspot, Cerrado's seasonal
131 precipitation regime is closely tied to the South American Monsoon System (Myers et al.,
132 2000; Grimm, Vera and Mechoso, 2004). According to the Köppen–Geiger classification,
133 the region's climate is predominantly tropical savanna (Aw) with a rainy season from
134 October to April and a dry season from May to September (Peel et al., 2007; Oliveira et
135 al., 2021). Annual rainfall ranges from 600 mm to 2,000 mm, with the highest averages
136 near the Amazon border and the lowest near the Caatinga, and the mean annual
137 temperature is 20.1°C (Sano et al., 2019).

138



139

140 Fig. 1: Map representing the distribution of Brazilian biomes according to IBGE (2024)
 141 and photos showing their general appearances. Amazon photo by Andre Deak, Pantanal
 142 photo by Leandro de Almeida Luciano, Pampa photo by Ilsi Boldrini, Caatinga photo by
 143 Matheus Andrietta, Cerrado photo by Jéssica Schüler, and Atlantic Forest photo by Tânia
 144 Rego.

145

146 Historically, the biome is subject to periodic fires, especially in the grassland and
 147 savanna formations, highly influencing the evolution of its vegetation (Simon et al., 2009;
 148 Simon and Pennington 2012). Currently, fires predominantly occur at the end of the dry
 149 season, during September and October (Gomes et al., 2020; MapBiomass Fogo 2024). The
 150 vegetation in the Cerrado can be classified into three main vegetation formations: Forests,
 151 Savannas and Grasslands. Forest formations predominantly consist of trees forming a
 152 continuous canopy, typically found on deeper soils (Ribeiro and Walter 2008). Savanna
 153 formations are defined by the presence of both arboreal and herbaceous-shrub strata with

154 a canopy cover ranging from 5% to 70% and tree heights reaching 8 m on average (Ribeiro
155 and Walter 2008). Finally, grassland formations consist of shrubs and sub-shrubs
156 intermixed with herbaceous strata (Ribeiro and Walter 2008).

157

158 **2.2 Model description**

159 The LPJmL-VR-SPITFIRE model is a fire-enabled DGVM that integrates the latest
160 version of the DGVM LPJmL (LPJmL 5.7, Wirth et al., 2024) with the most recent
161 improvements of the SPITFIRE fire regime model (Thonicke et al., 2010; Oberhagemann
162 et al., 2025), together with the variable-roots (VR) developed by Sakschewski et al.,
163 (2021). This model framework enables the simulation of global vegetation dynamics,
164 including the influence offire disturbance (Schaphoff et al., 2018; Drüke et al., 2019).

165 LPJmL simulates the growth and productivity of both natural and managed vegetation,
166 considering water, carbon, and energy fluxes, and represents vegetation through PFTs
167 (Schaphoff et al., 2018). The model accounts for factors such as climate, soil, water, and
168 nutrient availability to simulate the distribution, biomass, and productivity of PFTs, and
169 has been validated against observational data on productivity, biomass, evapotranspiration
170 and PFT distribution on the global scale (Schaphoff et al., 2018). We briefly outline only
171 the most important features of the LPJmL-VR-SPITFIRE model version, while referring
172 to Schaphoff et al., (2018) for the general LPJmL model description.

173 *Variable roots:* In the original LPJmL model, a PFT-specific shape parameter β defines
174 tree rooting depth and fine root biomass distribution (Jackson et al., 1996). To better reflect
175 the diversity of rooting strategies of tropical trees, Sakschewski et al., (2021) introduced a
176 range of possible rooting strategies (shallow to deep rooted trees) per PFT, that can coexist
177 or outcompete each other. Unless constrained physically by soil depth or by available
178 resources, actual rooting depth is scaled with tree height via a logistic root growth function,

179 and new carbon pools (root sapwood and heartwood) represent the plant's investment in
180 growing coarse roots (Sakschewski et al., 2021). A long-term selection of the best suited
181 rooting strategies amongst each PFT is mediated by a modified tree establishment
182 approach, where the most successful rooting strategies can produce more saplings.

183 *Water-stress mortality*: Tree mortality in LPJmL depends on tree longevity, growth
184 efficiency and heat stress (Schaphoff et al., 2018). In this study, a new mortality component
185 reflecting mortality risk due to water stress has been included. This newly integrated water
186 stress mortality depends on tree phenology (*phen*) (Forkel et al., 2014, applied in
187 Schaphoff et al., 2018), leaf senescence due to water stress (*phen_{water}*) and PFT-specific
188 parameters representing water stress resistance (*c_{res}*) and sensitivity to drought (*c_{sens}*).

$$189 \quad mort_{water} = c_{sens} \cdot phen \cdot (1 - phen_{water} - c_{res}) \quad (1)$$

190 *c_{sens}* is a PFT-specific parameter that determines the overall sensitivity to drought stress.
191 *Phen* represents the actual phenological state of a tree, ranging from 0 (no leaf cover) to 1
192 (full leaf cover). This term accounts for the fact that trees with lower phenology (i.e., more
193 dormant trees) experience reduced water stress mortality. The expression $(1 - phen_{water})$
194 represents the intensity of leaf senescence due to low water availability (Forkel et al.,
195 2014), indicating that periods of reduced water availability lead to higher drought-induced
196 mortality. *c_{res}* defines a threshold below which drought-induced leaf senescence does not
197 significantly impact tree survival.

198 This model refinement allows for a more accurate representation of PFT-specific
199 sensitivity to water stress. Coupled with the variable rooting scheme, LPJmL-VR-
200 SPITFIRE allows trees to optimize the trade-off between carbon investment in deep roots
201 and aboveground growth, providing a survival advantage under drought conditions. The
202 PFT-specific parameters are found in Table 1.

203 *SPITFIRE* is a process-based fire model that simulates wildfire occurrence, spread, and
204 behavior, while considering fuel availability, fuel composition and weather conditions to
205 simulate ignitions, rate of spread and flame intensity (Thonicke et al., 2010). By coupling
206 *SPITFIRE* into LPJmL-VR (LPJmL-VR-*SPITFIRE*), *SPITFIRE* can simulate the
207 influence of fire on vegetation dynamics. Vegetation properties simulated by LPJmL-VR,
208 such as PFT composition and litter fuel moisture, determine the simulation of fire spread
209 and intensity which in turn influence post-fire vegetation conditions. *SPITFIRE* considers
210 both human-induced and natural ignitions, with the likelihood of these ignitions
211 developing into fires depending on the fire danger index of the modelled grid cell. Fires
212 then spread depending on factors such as dead and live fuel composition, wind speed, and
213 fuel moisture. We adopted the VPD (water vapor pressure deficit)-dependent calculation
214 of the fire danger index (Drücke et al., 2019; Gomes et al., 2020b) and the most recent
215 updates to the fire spread functions (Oberhagemann et al., 2025). Both the fire danger
216 index and rate of spread calculations include PFT-specific parameters that reflect different
217 vegetation related properties that affect ignition, fire duration and propagation. Fire-related
218 tree mortality is calculated considering PFT specific bark thickness (influencing cambial
219 damage) and scorch height (influencing crown mortality). Furthermore, with the recent
220 updates, *SPITFIRE* allows for multi-day fires and considers moisture of the live grass
221 share. *SPITFIRE* feeds back to the vegetation components by calculating fire effects on
222 the vegetation, such as fuel combustion and post-fire tree mortality (Drücke et al., 2019;
223 Oberhagemann et al., 2025).

224

225 ***2.3 Parameterization of a new Savanna tree PFT***

226 The Cerrado trees exhibit considerable morphological and physiological differences
227 compared to other tropical forest trees growing in closed canopy and wet environments. In

228 LPJmL, these forests are represented by the Tropical Broadleaved Evergreen Tree PFT
229 (TrBE), reflecting the Amazon and the Atlantic rainforests, and by the Tropical
230 Broadleaved Raingreen Tree PFT (TrBR), representing seasonal closed forests. In contrast,
231 Cerrado vegetation is shaped by allometric relationships, and traits such as wood density,
232 specific leaf area (SLA), rooting depth, and bark thickness, which together create a
233 distinctive vegetation structure and functioning highly adapted to seasonal drought and fire
234 occurrence. To incorporate these characteristics into the LPJmL-VR-SPITFIRE model, we
235 used a combination of literature data and field observations to derive and calibrate the
236 relevant parameters for the new Tropical Broadleaved Savanna tree (TrBS)
237 parametrization. A summary of all parameters and data sources used is provided in Table
238 1 and 2, with detailed explanations below.

239 *2.3.1 Allometry and growth form*

240 The tree allometry is defined through a diameter distribution that follows an asymptotic
241 pattern, where height increases at a slower rate as diameter grows larger, with most trees
242 remaining under 10 meters in height (Fig. S2A and C). A similar trend is observed in the
243 relationship between diameter and crown area: trees initially grow in diameter,
244 subsequently expanding their crown until crown growth reaches a plateau (Fig. S2B and
245 D). This observed growth pattern is implemented by allometric relationships using PFT-
246 specific allometric parameters within the LPJmL model (Schaphoff et al., 2018; Eqn. S1;
247 Eqn. S2). To ensure an accurate representation of TrBS's tree growth, we analyzed field
248 data to estimate maximum height, maximum crown area, and their relationship with stem
249 diameter (Table S2). Using these field measurements, we derived the allometric constant
250 values that best aligned with the observed data, by fitting the allometric equations to the
251 data (Fig. S2). Details about site location, data collected, and their references can be found
252 on Table S2.

253 Despite variations of wood density and SLA due to factors such as soil quality,
254 temperature, and water availability, trees in more arid environments typically develop
255 denser wood with lower SLA values (indicating thicker leaves), an adaptation to water
256 scarcity and mechanical stress (Scholz et al., 2008; Terra et al., 2018, Souza et al., 2024).
257 While we based our wood density value on literature (Souza et al., 2024), the SLA values
258 used in the development of TrBS PFT were estimated from field data collected from 71
259 individuals of 26 species (Table 1, Table S2).

260
261 Table 1: Allometry, drought mortality and rooting parameters used to define the new
262 Tropical Broadleaved Savanna Tree (TrBS) PFT, along with the corresponding values for
263 the Tropical Broadleaved Evergreen Tree (TrBE), and Tropical Broadleaved Raingreen
264 Tree (TrBR). References cited apply exclusively to TrBS PFT. Details about the field
265 survey data are available on Table S2. Additional information on TrBE and TrBR
266 parameters, as well as parameters not included in this table, can be found in Schaphoff et
267 al., (2018).

Parameter	Tropical Broadleaved Evergreen tree	Tropical Broadleaved Raingreen tree	Tropical Broadleaved Savanna tree	Reference
Specific Leaf Area (SLA) ($\text{mm}^2 \cdot \text{mg}^{-1}$)	9.04	14.71	7.36	Field survey (Table S2)
Wood density ($\text{g} \cdot \text{cm}^{-3}$)	0.44	0.44	0.6	Souza et al., (2024)
Max. height (m)	100	100	10	Field survey (Table S2)
Max.crown area (m^2)	25	15	10	Field survey (Table S2)

Parameter	Tropical Broadleaved Evergreen tree	Tropical Broadleaved Raingreen tree	Tropical Broadleaved Savanna tree	Reference
Parameter in allometry function ($K_{allom\ 1}$)	100	100	153	Field survey (Table S2)
Parameter in allometry function ($K_{allom\ 2}$)	40	40	12	Field survey (Table S2)
Parameter in allometry function ($K_{allom\ 3}$)	0.67	0.67	0.52	Field survey (Table S2)
Maximum leaf-to-root-mass-ratio scaling parameter (lr_{max})	1	1	0.7	
Vertical root distribution parameter (β_{root})	[0.9418, 0.9851, 0.9925, 0.9950, 0.9963, 0.9971, 0.9976, 0.9981, 0.9986, 0.9993]			Sakschewski et al., (2021)
Shape parameter in logistic root growth function (k_{root})	0.02	0.02	0.07	Saboya and Borghetti (2012)

268

269

2.3.2 Root growth and belowground carbon allocation

270

Rooting depth is a crucial adaptation for the Cerrado species, enabling access to deep water reserves during prolonged dry periods (Oliveira et al., 2005; Tumber-Dávila et al., 2022). Due to its high investment in belowground structures, the Cerrado is often referred to as an 'upside-down forest,' storing approximately five times more carbon below-ground (in roots and as soil carbon) than above-ground (Terra et al., 2023). While deep roots are a well-documented feature of the Cerrado plants, rooting strategies vary widely among species. To try to reflect this diversity in rooting strategies in LPJmL-VR-SPITFIRE we

271

272

273

274

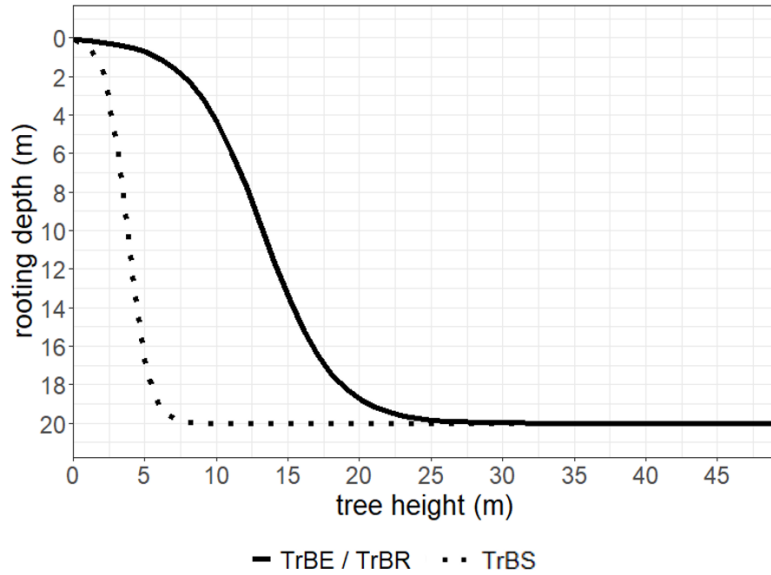
275

276

allowed for 10 different root distributions (β_{root} parameter) per PFT. We chose the same range of β_{root} values for TrBS PFT as for the other PFTs, to allow a spectrum of shallow, intermediate and deep rooting strategies to compete. From β_{root} the depth where 95% of root biomass are found (D95) can be calculated (see Sakschewski et al., 2021). Studies show that the Cerrado tree seedlings invest more in root growth compared to shoot growth as a strategy to access water deeper in soil during the dry season (Hoffmann, Orthen and Franco 2004; Saboya and Borghetti 2012). We reflect this by modifying the shape parameter of the logistic root growth function (k_{root} , Table 1), to allow TrBS to reach deeper rooting depths earlier in their lifecycle (Fig. 2), enhancing the underground competitiveness of these savanna trees. In LPJmL-VR-SPITFIRE, carbon allocation to coarse woody roots is represented by separate root sapwood and heartwood carbon pools, introduced in addition to the fine root carbon pool (Sakschewski et al., 2021). Due to the necessary balance between root and stem sapwood investment (Pipe Model approach; Shinosaki et al., 1964), and the relationship between tree height and rooting depth, deep root growth for TrBS saplings represents a trade-off between above- and belowground growth.

The ratio between the leaf and the fine root biomass in the model depends on the model internally calculated water stress index (ω), where more root biomass is built under water stress, and is constrained by the lr_{max} (maximum leaf-to-root-mass-ratio) scaling parameter (Table 1; Schaphoff et al., 2018). We set lr_{max} to 0.7 to allow TrBS to invest relatively more into root biomass than the other tropical tree PFTs, where lr_{max} was set to 1 (Schaphoff et al., 2018).

299



300

301 Fig. 2: Logistic growth function scaling rooting depth to tree height, shown for a soil depth
 302 of 20m for the different PFTs (TrBE = tropical broadleaved evergreen, TrBR = tropical
 303 broadleaved raingreen, TrBS = Tropical Broadleaved Savanna).

304

305 *2.3.2 Phenology*

306 The Cerrado exhibits pronounced precipitation seasonality, which shapes the
 307 phenology of its vegetation. Deciduous and semi-deciduous species display leaf dynamics
 308 in which leaves shed during the dry season, peaking in July, and sprout during the
 309 transition to the rainy season in September (de Camargo et al., 2018). Despite the
 310 dominance of deciduous and semi-deciduous species (74%), the community rarely
 311 experiences complete defoliation, retaining at least half of its foliage in most years (de
 312 Camargo et al., 2018). This seasonal pattern is also evident in the Leaf Area Index (LAI)
 313 of trees. LAI values drop from around 1 in the rainy season to approximately 0.6 on the
 314 peak of the dry season (Hoffmann et al., 2005).

315

316 The degree of foliation in LPJmL-VR-SPITFIRE is given by the phenology status,
 317 which is updated daily (ranging from 0 = no leaves to 1 = full leaf cover) and derived by
 multiplication of four limiting functions, namely a water-limiting (f_{water}), light-limiting

318 (f_{light}), cold-limiting (f_{cold}) and heat-limiting (f_{heat}) function (Schaphoff et al., 2018;
319 Forkel et al., 2014). The shape parameters of f_{water} were chosen to reflect a behaviour
320 intermediate between the evergreen and the raingreen PFT (Fig. S3), and thereby reflects
321 the general phenological behaviour of the Cerrado community as explained above; f_{heat} ,
322 f_{cold} and f_{light} were set to the same values as for TrBE.

323 *2.3.4 Fire dynamic and vegetation adaptation*

324 Over 10.5 million hectares burned in the Cerrado in 2024 (MapBiomas Fogo 2025),
325 with 98% of these fires attributed to human activity (Schumacher et al., 2022). At local
326 and landscape scales, fire dynamics are influenced by factors such as fuel availability,
327 ignition sources, topography, and climatic conditions (Gomes, Miranda, and Bustamante
328 2018). In the Cerrado, fire behavior is closely tied to seasonal cycles and one key factor
329 determining its behavior is the vapor pressure deficit (VPD) (Gomes, et al., 2020b; Oliveira
330 et al., 2021). VPD is the measure of the difference between the vapour pressure of the
331 moisture present in the air and the maximum vapour pressure the air can hold, being
332 influenced by temperature and relative humidity. In the Cerrado, the VPD varies
333 seasonally, with average values around 0.3 to 0.7 kPa in the rainy season and 1.4 to 2.0
334 kPa in the dry season (Cattelan et al., 2024). Higher VPD dehydrates plant biomass,
335 especially from grasses, making it more flammable and susceptible to fire (Gomes, et al.,
336 2020b). The VPD affects the rate of spread and intensity of the fire, with higher VPD
337 resulting in faster and more intense fires in a given fuel bed (Gomes et al., 2020b; Oliveira
338 et al., 2021). In LPJmL-VR-SPITFIRE, the fire danger index depends on VPD and is
339 scaled via a PFT-specific factor α VPD, where higher values of α VPD increase fire danger.
340 We calibrated α VPD to achieve good agreement between observed and modelled burnt
341 area. A higher α VPD for TrBS than for TrBE and TrBR was chosen, because the fuel

342 produced by the Cerrado trees burns more readily, compared to the fuel dropped by trees
343 in the moist forests (dos Santos et al., 2018).

344 Because of its fire-prone environment, the Cerrado trees exhibit several adaptations that
345 enable them to survive fire damage. These include belowground organs that promote
346 resprouting after fire, thick bark that insulates and protects internal tissues, robust terminal
347 branches, leaves concentrated at branch tips, and persistent stipules that safeguard apical
348 buds, all minimize fire damage (Simon et al., 2009; Simon and Pennington 2012). Fire-
349 induced tree mortality in LPJmL-VR-SPITFIRE results from combined effects of cambial
350 and crown damage (Oberhagemann et al., 2025). PFT-specific parameters for bark
351 thickness were chosen to fit the relationship between stem diameter and bark thickness
352 shown in Hofmann et al., (2009) (Fig. S3; Table 2). Scorch height, the highest point at
353 which flames reach and affect the vegetation, is calculated from fire intensity and a PFT
354 specific scaling factor (F ; see Eqn. S5), which also depends on tree crown length relative
355 to its height (Thonicke et al., 2010; Oberhagemann et al., 2025). The Cerrado trees have
356 relatively long crowns compared to their total height, with a ratio of 0.53 (Table 2). While
357 this exposes them to crown scorch, the above-mentioned adaptations result in an overall
358 lower mortality risk from crown scorch, and we therefore adjusted the parameter F
359 accordingly (Table 2).

360
361
362
363
364
365

366 Table 2: Fire parameters used to define the new Tropical Broadleaved Savanna Tree
 367 (TrBS) PFT, along with the corresponding values for the Tropical Broadleaved Evergreen
 368 Tree (TrBE) and Tropical Broadleaved Raingreen Tree (TrBR) PFTs. References cited
 369 apply exclusively to TrBS PFT. SPITFIRE parameters for TrBE and TrBR are taken from
 370 (1) Thonicke et al., (2010), and (2) Drüke et al., (2019).

Parameter	Tropical Broadleaved Evergreen tree	Tropical Broadleaved Raingreen tree	Tropical Broadleaved Savanna tree	Reference
Leaf Longevity (years)	1.6	0.5	1	Cianciaruso et al., (2013); Souza, J. P. (2012)
Sensitivity to drought (c_{sens})	100	100	10	
Water stress resistance (c_{res})	0.1	0.1	0.1	
Water limitation factor ($wscal_{min}$)	0	0.35	0	
α VPD	6	6	10	
Crown length parameter	0.3334 ₍₁₎	0.10 ₍₁₎	0.53	Field survey (Table S2)
Scorch height parameter (F)	0.193 ₍₂₎	0.0799 ₍₂₎	0.13	
Bark thickness par1/par2	0.0301/0.0281 ₍₁₎	0.1085/0.212 ₍₁₎	0.135/0.2820	Hoffmann et al., (2009)

372 **2.4 Simulation protocol**

373 To evaluate the performance of the newly implemented TrBS PFT, two simulation runs
374 were conducted: one including TrBS PFT (hereafter ‘Savanna’ simulation) and the other
375 experiment excluding it (hereafter ‘No Savanna’ simulation). Both simulations covered
376 the period from 1901 to 2019, with a 5000-year spin-up phase, and utilized identical
377 environmental input data in a 0.5° horizontal resolution.

378 The model spin-up was simulated from bare ground using climate input from 1901-
379 1930 (with pre-industrial $p\text{CO}_2 = 276.59 \text{ ppm}$), which was repeated for 5000 years, to
380 allow carbon pools to reach equilibrium with climate. The transient simulation then ran
381 from 1901 to 2019. For model validation, we analyzed the last 30 years of the transient
382 run. Because we aim to evaluate the establishment and general characteristics of the new
383 TrBS PFT, all simulations were conducted for potential natural vegetation (PNV) only,
384 with no simulation of human land use to focus on geographical distribution of vegetation
385 and fire. While LPJmL-VR-SPITFIRE features the latest model updates regarding the
386 nitrogen cycle (Blohm et al., 2018) and biological nitrogen fixation (Wirth et al., 2024), we
387 switched the nitrogen limitation off as it was beyond the scope for this study.

388 The LPJmL-VR-SPITFIRE model uses daily climate input, including air temperature,
389 precipitation, wind speed, humidity, and long- and shortwave radiation. These datasets
390 were sourced from ISIMIP3a (<https://data.isimip.org/10.48364/ISIMIP.664235.2>), which
391 combines GSWP3 data (1901–1978) and W5E5 data (1979–2019). Atmospheric CO_2
392 concentration data were derived from the TRENDY project (Friedlingstein et al., 2023).

393 Soil texture data were obtained from the Harmonized World Soil Database
394 (Nachtergaele et al., 2009). Soil depth in LPJmL-VR-SPITFIRE was defined using the
395 lower water table depth values provided by the SOIL-WATERGRIDS dataset (Guglielmo
396 et al., 2021).

397 Ignition sources for the SPITFIRE model are based on population density (Klein
398 Goldewijk et al., 2011) for human ignitions, and lightning occurrence data from the
399 OTL/LIS dataset (Christian et al., 2003) for natural ignitions.

400

401 **2.5 Model validation**

402 For each of our simulation outputs, we selected appropriate Brazilian or global datasets
403 to validate the modeled results from LPJmL-VR-SPITFIRE. All spatial analysis and
404 comparisons between the validation data and model outputs were conducted in R, utilizing
405 the ncdf4, terra, raster and sf packages. The analysis focused on the mean values of the last
406 30 years of the simulations (1990-2019). Details of each validation dataset are provided
407 below.

408 *2.5.1 Vegetation distribution*

409 To validate the modeled distribution of the vegetation in Brazil, represented by the
410 foliar projected coverage (FPC) of each PFT, we used Brazil's original vegetation
411 distribution by IBGE (2017). The original IBGE map was a very detailed Shapefile, with
412 specific variation of each major vegetation group, that would have complicated the
413 comparison with the FPC and limited number of PFTs. For this reason, we aggregated the
414 vegetation classes into 13 vegetation types following the attribute table of IBGE's product
415 (Fig. 4). After that, we converted the Shapefile into a raster file using the function rasterize
416 from the terra package in R.

417 To evaluate the distribution of the new TrBS PFT, as well as the other tropical PFTs,
418 we overlaid the FPC output with the corresponding classification from IBGE. For this
419 comparison, we selected only grid cells where the respective $FPC \geq 0.3$ and matched the

420 class in the IBGE dataset, generating a map that identifies under-, over-, and correctly
421 simulated PFT coverage.

422 *2.5.2 Above- and belowground Biomass, evapotranspiration and productivity*

423 The above- and belowground biomass (AGB and BGB) validation maps were produced
424 by the team from the Fourth National Communication to the United Nations Convention
425 of Climate Change, here referred to as QCN (MCTI 2020). These maps were produced
426 considering the distribution of Brazil's original vegetation (IBGE 2017) and estimating
427 AGB and BGB using specific equations and field data that best fit each vegetation type.
428 From these maps we derived a BGB:AGB ratio map to validate the structural
429 characteristics of TrBS PFT. For better comparison, we calculated the Spearman
430 Correlation between the two modeled scenarios of BGB:AGB and the QCN validation
431 using the stats package from R software.

432 For evapotranspiration (ET) and gross primary productivity (GPP), the mean annual
433 distribution of the last 30 simulation years (1990-2019) were compared to reference
434 datasets (GPP: Carvalhais et al., 2014; ET: ERA5, Hersbach et al., 2020) and evaluated
435 via the Normalized Mean Squared Error (NMSE) and Pearson correlation (as described in
436 Sakschewski et al., 2021).

437 *2.5.3 Burned Area*

438 The Burned Area validation map was produced using the annual burned coverage
439 product from MapBiomas Fogo 3.0 (2024) database. This product gives a 30 m resolution
440 presence-absence map of areas in which fire occurred for a time series from 1985 to 2023.
441 The burned area was calculated from the burned coverage for a 0.5° grid, covering all the
442 Brazilian territory, for each year from 1990 to 2019. Then, from resulting annual burned

443 area maps, we calculated the mean burned area for all selected time series. All calculations
444 and map generation from the MapBiomas dataset were performed using the Google Earth
445 Engine platform.

446 For the spatial distribution of annual burned area, we created a map of the human land-
447 use fraction based on MapBiomas 9.0 land-use data (MapBiomas, 2024), using the mean
448 value from 1990 to 2019 (Fig. S5). Since our simulation considers only potential natural
449 vegetation (PNV), we weighted the burned area, in both the validation data and model
450 output, to account for fire occurrences in human-managed land.

451 The validation of the monthly burned area for the Cerrado biome was conducted using
452 the MapBiomas Fogo 3.0 dataset (2024). The burned area validation was also weighted by
453 the natural land-cover of the corresponding year. This dataset was used to assess the
454 accuracy of the simulated seasonal burned area patterns in the Cerrado. The comparison
455 between the simulated scenarios and the MapBiomas data was evaluated using Normalized
456 Mean Squared Error (NMSE), Willmott's index, R^2 , and p-value statistics from the
457 respective R packages kerntools, hydroGOF and stats (Drücke et al., 2019).

458 For carbon emission by fire (FireC), our validation is based on the Global Fire
459 Emissions Database (GFED4), which derives its fireC emission maps using its own burned
460 area data (van der Werf et al., 2017). GFED4 combines satellite observations of burned
461 area with biogeochemical modeling to estimate emissions of CO₂, CO, CH₄, and other
462 trace gases. Given the strong link between burned area and fire emissions, we apply the
463 same land-use fraction weighting approach as for burned area to ensure consistency in our
464 analysis.

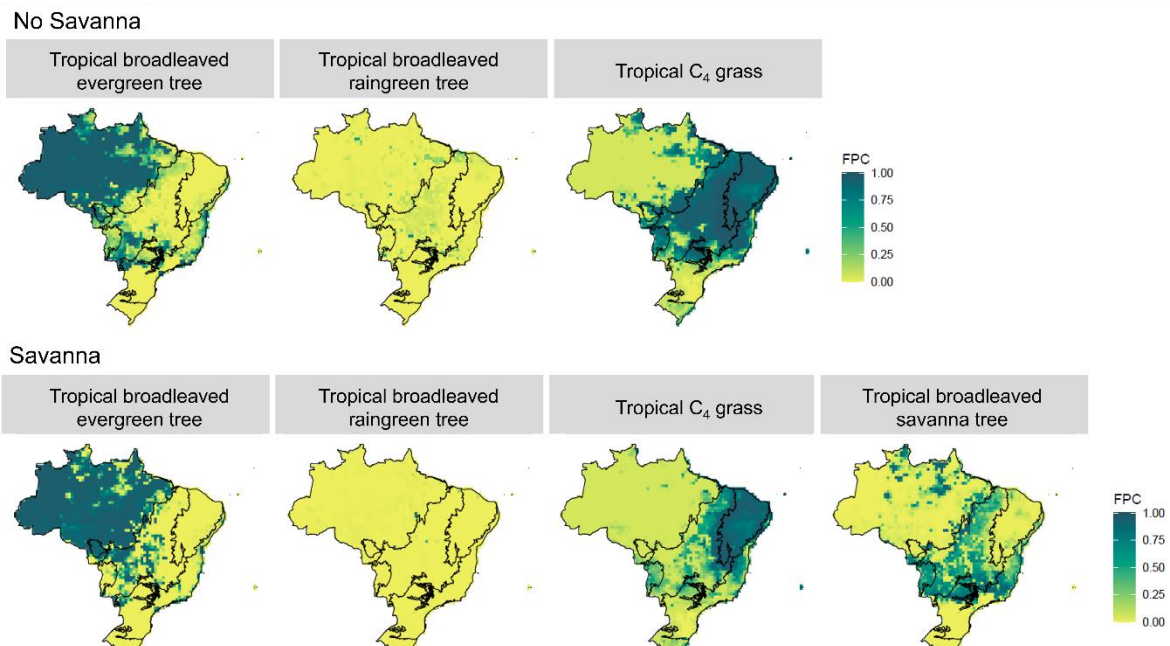
465 **3. Results**

466 ***3.1 Vegetation distribution***

467 The inclusion of TrBS PFT and the implementation of the Drought Mortality
468 Function have significantly altered the distribution and abundance of key vegetation
469 types across Brazil, particularly the Tropical C₄ grasses and TrBE PFTs (see the
470 supplementary file for further information). In simulations without TrBS, C₄ grass
471 dominates across northeastern and central Brazil, occupying the whole Caatinga biome,
472 most of the Cerrado and northern Atlantic Forest (Fig. 3).

473 TrBS establishes itself predominantly in the Cerrado and Pantanal biomes, aligning
474 with regions classified as savanna vegetation by IBGE (Figs. 3 and 4). Pockets of TrBS
475 also appear in northern portions of the Amazon biome, where patches of savanna-like
476 vegetation can occur, and Atlantic Forest regions where seasonal forest is present (Fig.
477 3 and 4). The presence of TrBS results in a contraction of C₄ grass, which retreats mostly
478 to the Caatinga biome, where they almost entirely dominate due to Caatinga's dry
479 environment, while grass and savanna vegetation coexist in Pantanal, northern and
480 eastern Cerrado (Fig. 3).

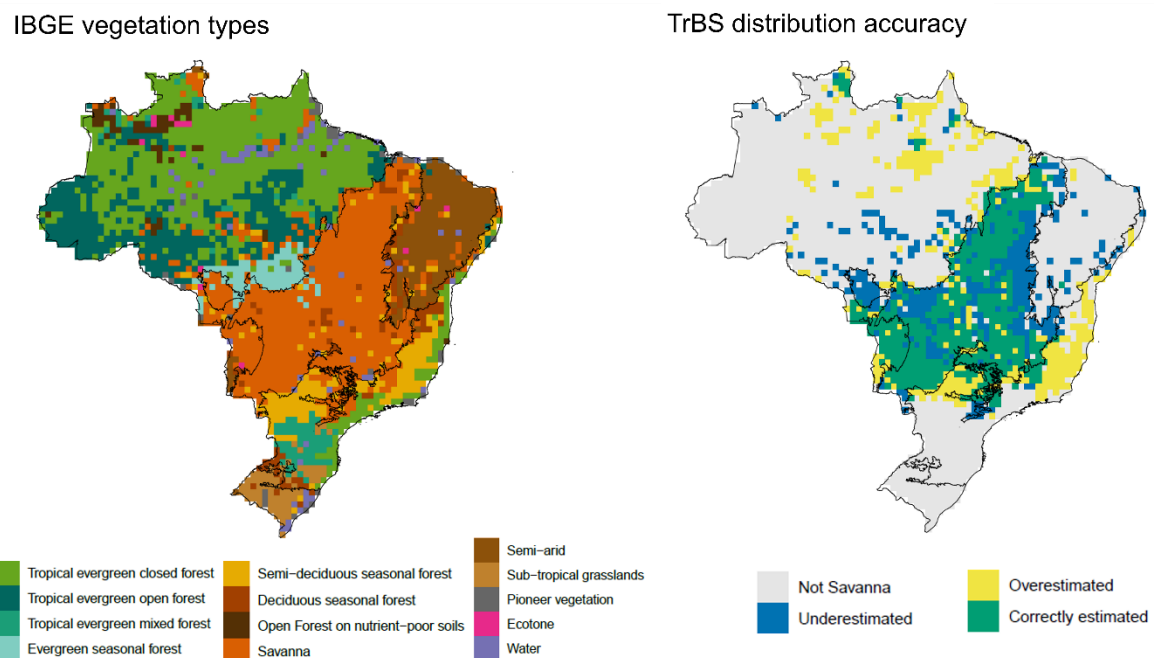
481



482

483 Fig. 3: Foliar Projected Cover (FPC) of the Plant Functional Types (PFT) for Tropical
484 Broadleaved Evergreen Tree, Tropical Broadleaved Raingreen Tree, Tropical C₄ Grass
485 and Tropical Broadleaved Savanna Tree in Brazil under two model configurations: 'No
486 Savanna' and 'Savanna'.

487



488

489 Fig. 4: Maps showing the Brazilian vegetation types according to IBGE (left) and TrBS
490 PFT distribution accuracy (right) in comparison with the savanna vegetation class from
491 IBGE. A threshold of 30% FPC cover was used to determine distribution accuracy.

492

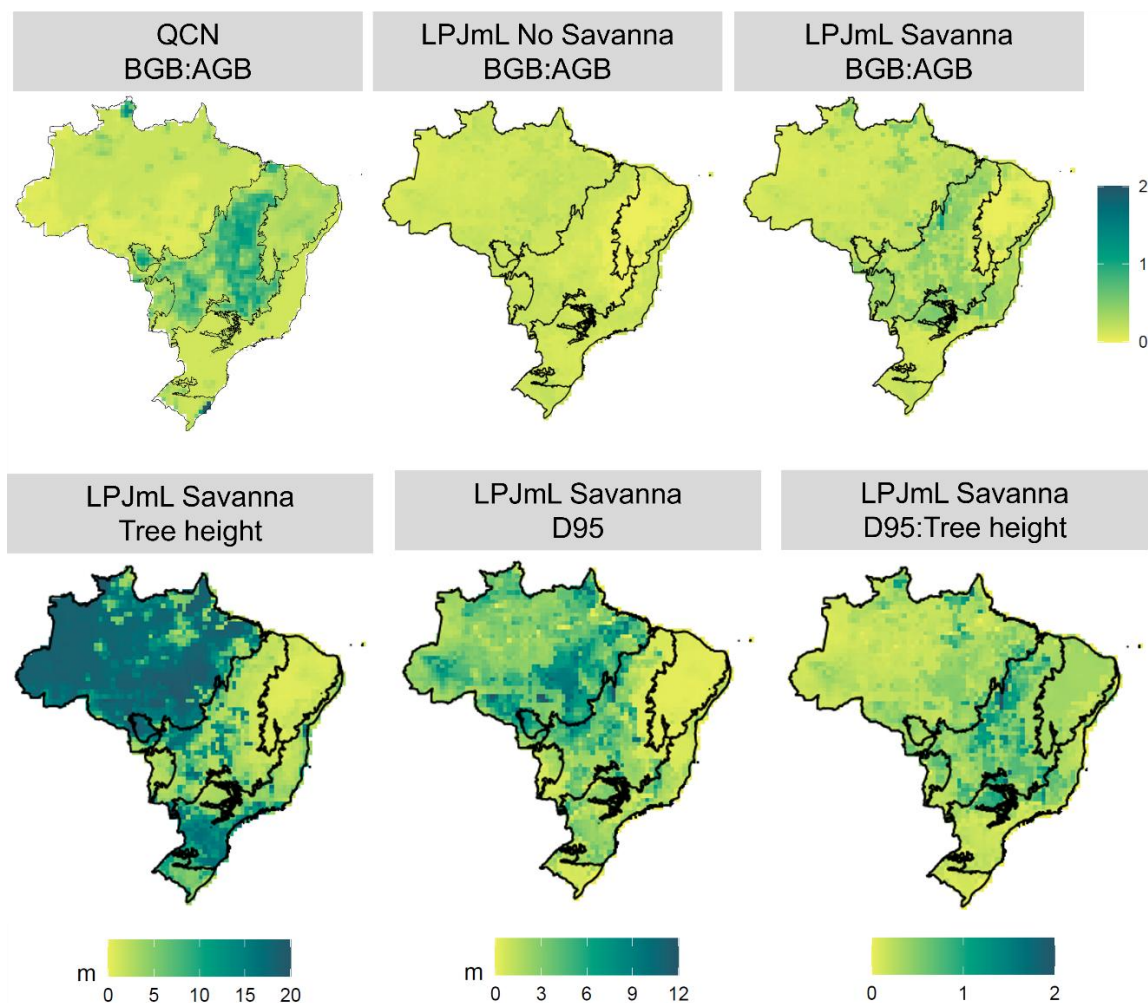
493 **3.2 Above- and belowground Biomass and vegetation structure**

494 The inclusion of TrBS PFT significantly improved the simulated above- and
495 belowground biomass patterns across Brazil compared to simulations without it. By better
496 capturing the characteristic small trees with extensive belowground structures of the
497 Cerrado, TrBS PFT led to an improved representation of the 'upside-down forest' in central
498 Brazil (Fig. 5). As a reflection of the distinct allocation strategies of the Cerrado
499 vegetation, the biomass ratio (BGB:AGB) was also clearly improved in the Savanna
500 scenario (Fig. 5). Although the simulated values did not fully match those observed in the
501 QCN validation, as shown by the Spearman correlations (QCN vs. Savanna: 0.27; QCN
502 vs. No Savanna: -0.16), the introduction of TrBS resulted in a more accurate simulation of
503 carbon allocation across Brazil. Both scenarios also showed good performance relative to
504 the reference data for GPP (NMSE < 1), with the Savanna model having a marginally lower
505 error compared to the No Savanna (Fig. S10; Table S3). For ET, deviations from the
506 validation dataset are large for both scenarios, with the No Savanna having a slightly better
507 performance (NMSE = 1.56) compared to the Savanna (NMSE = 1.89) (Fig. S10; Table
508 S3).

509 TrBS PFT also improved the representation of tree height gradients, with tall trees,
510 above 20 m, in the Amazon transitioning to slightly shorter trees in the southern Amazon
511 and reaching approximately 7 m in the Cerrado (Fig. 5; Fig. S7). Additionally, the model
512 now captures a gradient in rooting depth (D95), with shallower roots in the Amazon,
513 deepening towards the southern Amazon and Cerrado (Fig. 5; Fig. S7). This pattern is

514 further supported by a higher D95:height ratio in the Cerrado, aligning with the
515 characterization of its vegetation as an 'upside-down forest,' where rooting depth can
516 exceed tree height.

517



518

519 Fig. 5: FPC-weighted BGB:AGB below- and aboveground biomass ratio (BGB:AGB)
520 from LPJmL simulations and QCN validation product (top row), and FPC-weighted tree
521 height and D95, and their ratio (D95:Tree height) from LPJmL 'Savanna' simulation
522 (bottom row).

523

524 **3.3 Fire dynamics**

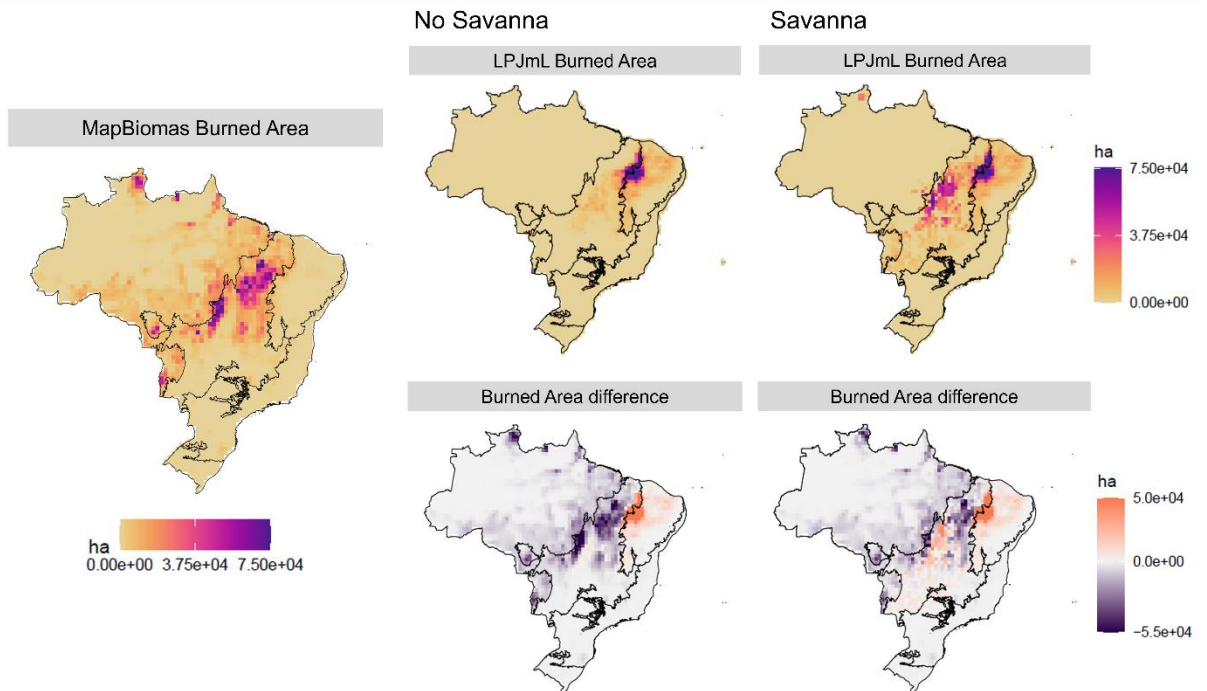
525 The introduction of TrBS PFT significantly influenced burned area patterns across
526 biomes. LPJmL-VR-SPITFIRE generally underestimated burned areas in the ‘No
527 Savanna’ simulation, particularly in the Cerrado and Amazon regions, while
528 overestimating them in the Caatinga (Table 3; Fig. 6). With the inclusion of the new TrBS
529 PFT, the burned area estimates in the Cerrado increased, surpassing the values recorded in
530 the MapBiomas Fogo in central Cerrado, but still underestimating burned area in the
531 northern region of Cerrado and in the Amazon (Fig. 6). Despite these regional
532 discrepancies and given the SPITFIRE improvements applied to both model
533 configurations, the inclusion of TrBS PFT and its adjusted parameterizations led to a clear
534 improvement in the total burned area estimates for Brazil (Table 3).

535
536 Table 3: Total burned area for all Brazilian biomes simulated by LPJmL-VR-SPITFIRE
537 for ‘Savanna’, and ‘No Savanna’ scenarios, and the validation data from MapBiomas
538 Fogo. The values are in Thousand hectares (Kha).

	Savanna (Kha)	No Savanna (Kha)	MapBiomas (Kha)
Cerrado	6660.7	2597.21	7748.43
Amazon	405.67	44.48	4991.57
Atlantic Forest	89.69	5.82	130.83
Caatinga	2937.68	2818.43	345.6
Pantanal	203.84	5.33	558.55
Pampa	1.15	1.15	11.89
Brazil	10298.73	5472.42	13786.89

539

540



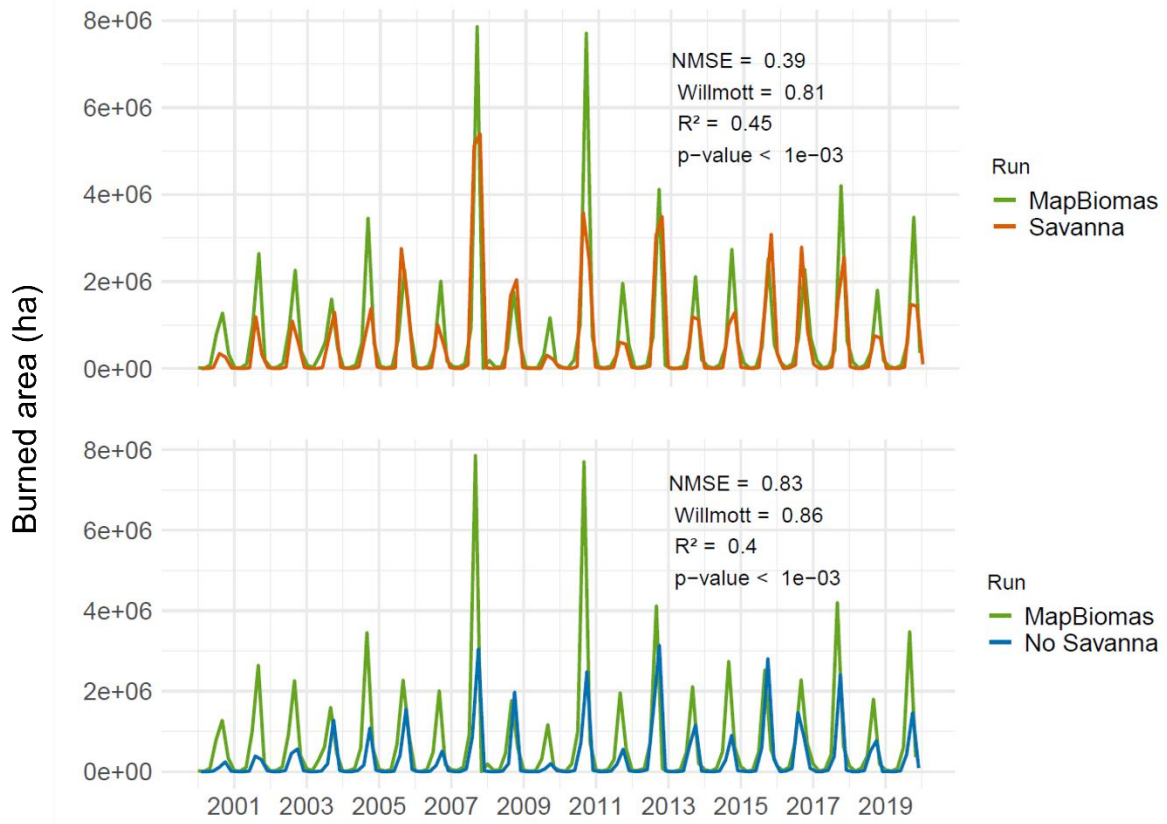
541

542 Fig. 6: LPJmL simulations of burned area in Brazil for ‘No Savanna’ and ‘Savanna’
 543 scenarios (top row), the validation data by MapBiomass Fogo (left), and the respective
 544 difference between simulated results and MapBiomass Fogo validation (bottom row).

545

546 We could also observe an improvement in the seasonal patterns of the burned area in
 547 the Cerrado Biome with the incorporation of TrBS PFT (Fig. 7). The Savanna scenario,
 548 compared to the MapBiomass data, shows an NMSE of 0.39 with an R^2 of 0.45, and a
 549 Willmott index of 0.81, indicating that the model has a good fit. The No Savanna scenario
 550 has a slightly higher NMSE (0.83) and Willmott index (0.86), and a lower R^2 (0.40)
 551 compared to MapBiomass, suggesting that removing TrBS reduces the overall model’s
 552 ability to represent observed seasonal fire patterns.

553



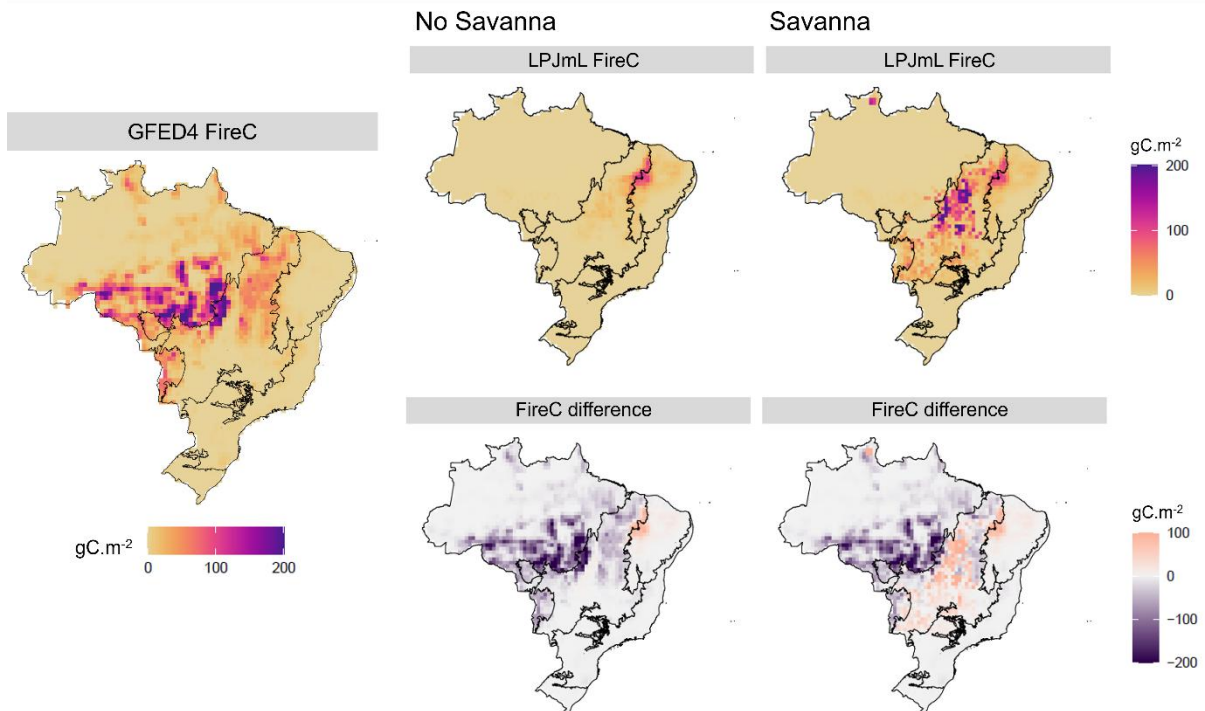
554

555 Fig. 7: Total monthly burned area, for the Cerrado Biome, from 2000 to 2019 for two
 556 LPJmL simulation scenarios: 'Savanna' (top) and 'No Savanna' (bottom) in comparison
 557 with the monthly burned area product from MapBiomas Fogo.

558

559 Carbon emission by fire (FireC) patterns reflect directly the burned area patterns (Fig.
 560 8). Overall, the introduction of TrBS did not improve emission estimates in Brazil as most
 561 of the emission comes from southeastern Amazon, which has its burned area highly
 562 underestimated by our model. In the Cerrado, fire-related emissions were overestimated in
 563 the Savanna scenario, particularly in the central part of the biome, reflecting the spatial
 564 patterns of burned area.

565



566

567 Fig. 8: LPJmL simulations of Fire carbon emission in Brazil for No Savanna
 568 scenarios (top row), the validation data by GFED4 (left), and the respective difference
 569 between simulated results and GFED4 validation (bottom row).

570

571 ***3.4 Extrapolation to the global scale***

572 Since the LPJmL-VR-SPITFIRE model will also be run on a global scale in future
 573 applications, the parameterization of the new PFT was tested in a global simulation using
 574 the same climate input data set as for the Brazilian simulations. Although TrBS PFT was
 575 specifically adapted to the Cerrado tree data, we found high agreement in the simulated
 576 global savanna distribution compared to a reference dataset (Hengl et al., 2018). The
 577 results are shown in Supplementary Fig. S9.

578

579 **4. Discussion**

580 ***4.1 Advancing in Savanna Modeling***

581 The introduction of a savanna-specific Plant Functional Type in the LPJmL-VR-
582 SPITFIRE model significantly enhances the representation of vegetation and fire dynamics
583 in Brazil. TrBS improved simulations of carbon allocation, particularly below- to
584 aboveground biomass ratio, and better represented fire behavior, especially the temporal
585 dynamics of burned area. Key features of the Cerrado, that also apply to tropical savannas
586 in general, are now well represented: a vegetation that is adapted to seasonal drought
587 environments by accessing water with deep root systems and allocating more resources
588 belowground and can cope with or even depends on regular occurring fires. This update
589 moves the capability of LPJmL-VR-SPITFIRE beyond the previous binary classification
590 of tropical rainforests and grasslands, allowing for a more nuanced depiction of ecological
591 transitions, such as the Amazon-Cerrado interface. By incorporating savanna vegetation,
592 the model facilitates more realistic investigations into the future dynamics of these biomes
593 and allows for a more critical evaluation of restoration efforts within this specific
594 vegetation type. A model limited to representing only 'forest' and 'grasslands' will fail to
595 capture the significance and vulnerabilities inherent in savanna ecosystems like the
596 Cerrado.

597 Other DGVMs have struggled earlier to accurately depict the savanna biome (Whitley
598 et al., 2017; Baudena et al., 2015), as many of them oversimplify root dynamics, specific
599 phenology and vegetation-fire feedback. In particular, the role of rooting depth, which is
600 often constrained to shallow values in DGVMs, has a significant impact on the competition
601 between forest, savanna vegetation and grasses, as shown by Langan et al., (2017) for
602 South America. The introduction of root growth and rooting depth diversity in the LPJmL
603 model (Sakschewski et al., 2021) can therefore be considered key to improving savanna

604 modeling, as it allows vegetation adaptation to water scarcity, especially when subdividing
605 the PFTs into different rooting strategies. Importantly, the competition for water between
606 savanna trees and grasses can also be better depicted when partitioning of access to water
607 resources is considered (Whitley et al., 2017; Baudena et al., 2015).

608 We parameterized the savanna tree PFT using field and literature data specific to the
609 Brazilian Cerrado region and achieved a good fit between modelled and observed savanna
610 distribution. Other modeling studies, for example Moncrieff et al., (2016), have
611 encountered challenges to capture the Cerrado extent due to missing processes.
612 Extrapolations of model parametrization that were specifically evaluated for one savanna
613 region, here the Cerrado, often leads to inaccuracies, given the distinct climate, species
614 composition, and fire-vegetation interactions in each of the savanna-type regions (Solbrig
615 et al., 1996; Lehmann et al., 2014; Moncrieff et al., 2016). Nevertheless, to assess the
616 robustness of our parameterization, we conducted a global simulation and found that the
617 parameterization developed for the Brazilian savanna performed well in simulating global
618 tropical savanna distributions (Fig. S9). Future work could also include an assessment to
619 better capture main functional differences between each savanna-type region.

620

621 ***4.2 Challenges in Representing the Cerrado Dynamics***

622 Despite these advancements, several challenges remain in capturing the complex
623 vegetation dynamics of the Cerrado. Although our simulations already produce a mix of
624 savanna trees and grasses in the northern Cerrado, one key issue is achieving a realistic
625 balance and dynamic feedback between tree and grass cover. Achieving a more realistic
626 vegetation structure is challenging with representing tree and shrub individuals as
627 generalized representatives of each PFT, even though differentiations by rooting depth
628 were incorporated in LPJmL-VR-SPITFIRE. Building on the knowledge gained in this

629 study a gap-model framework that simulates individual trees and also incorporates trait
630 diversity such as the LPJmL-FIT model (Sakschewski et al., 2015; Thonicke et al., 2020),
631 could offer a more accurate representation of tree-grass coexistence in the near future.

632 Our analysis focused on depicting the overall distribution and performance of the new
633 savanna PFT across Brazil. A detailed, site specific validation of carbon and water fluxes,
634 the seasonality of leaf cover and productivity might complement the results of this study.
635 In this context, further model refinement could be undertaken, such as implementing shade
636 intolerant PFTs in the model (Ronquim et al., 2003; Lemos-Filho et al., 2010).
637 Additionally, a notable limitation observed in our simulations is the overrepresentation of
638 C₄ grasses in the Caatinga biome, which contrasts with the known vegetation
639 characteristics of the region. The Caatinga is a semi-arid biome characterized by diverse
640 vegetation physiognomies, including succulents and small shrub vegetation, with a
641 predominance of seasonal dry tropical forests rather than extensive grasslands (de Queiroz
642 et al., 2017). As discussed for the tree-grass coexistence in the previous paragraph,
643 Caatinga vegetation modeling would benefit from an individual tree approach (as in
644 LPJmL-FIT) rather than the average individual approach of the LPJmL model. Addressing
645 this will be important for improving model realism and its applicability to drier tropical
646 ecosystems, as well as enhancing its performance in representing fire patterns in the region.

647 Fire impacts on the vegetation are a key process that maintains savannas' open-canopy
648 structure. Our parameterization of the savanna tree PFT resulted in a vegetation type with
649 high flammability, yet is well protected against lethal fire damage. However, resprouting
650 mechanisms, which are crucial for post-fire recovery (Souchie et al. 2017) are not yet
651 implemented explicitly in the vegetation model but would improve the simulation of
652 vegetation recovery. The amount of fuel available for burning is another key area of
653 ongoing model development, as it strongly influences fire spread and intensity. In the most

recent SPITFIRE version that we used in this study, the live grass moisture calculation was substantially improved (Oberhagemann et al., 2025), better reflecting seasonal dynamics of fuel availability of grass vegetation. Although the inclusion of the TrBS PFT may improve the representation of vegetation structure and total biomass in the Cerrado, we could not assess whether this translated into an improvement in fuel biomass estimates. In SPITFIRE, leaves and a proportion of sapwood and heartwood from twigs, branches, and trunks are considered to calculate living fuel biomass (Thonicke et al., 2010). QCN products, on the other hand, do not distinguish carbon stored in these specific tree components but only report total above- and belowground biomass; therefore, a direct validation or assessment of fuel biomass improvement resulting from the TrBS implementation was not feasible.

In Savannas, there is often extensive use of fire for land management purposes. Specifically, in the Cerrado, fire in natural areas is associated with the use of fire for deforestation and pasture management, with fire escaping to natural areas, while in areas of mechanized agriculture and planted forests, owners rather protect the areas against fire. In SPITFIRE, however, ignitions are represented solely as a function of population density, and the model does not explicitly capture the diverse fire management regimes common in these regions. This simplification contributes to the underestimation of burned area along the Caatinga border, where expanding deforestation and intensive land management interact with natural fire regimes, as well as in southeastern Amazonia, where large-scale pasture management fires may escape and affect adjacent rainforest (MapBiomas Fogo, 2024; Cano-Crespo et al., 2015). To mitigate this, we weighted both validation data and model outputs by the human land-use fraction from MapBiomas, thereby excluding grid cells with extensive anthropogenic land use from the analysis. Recent attempts to better incorporate anthropogenic fire management into models (Perkins et al., 2024) could

enhance Cerrado fire simulations, which is particularly relevant given the increasing pressures on the biome and the ongoing shifts in fire regimes (da Silva Arruda et al., 2024). Nevertheless, even with improved fire–vegetation dynamics, simulations of future trajectories of these dynamics will remain constrained if key vegetation traits, such as deep root water uptake, are not adequately represented (D’Onofrio et al., 2020; Baudena et al., 2015).

The most recent version of LPJmL incorporates the nitrogen cycle (von Bloh et al., 2018), along with mechanisms of biological nitrogen fixation (BNF, Wirth et al., 2024). Soils in the Cerrado are characterized by acidity, high aluminum concentrations, and nutrient scarcity (Bustamante et al., 2006; 2012), requiring vegetation to develop specific adaptations that confer a competitive advantage in these nutrient-poor conditions. Future advancements should leverage these model enhancements to incorporate nitrogen and other nutrient constraints, enhancing ecological realism to specifically address this aspect to the complex ecological interactions.

Beyond the factors already discussed, rootable soil depth significantly influences vegetation dynamics. However, determining the maximum depth roots can physically penetrate is challenging, as they can grow into bedrock and access groundwater, but are also limited by high soil density and low oxygen availability. In our simulations we used the water table depth of Guiglemo et al., (2021) as a proxy for rootable soil depth, which allows deep rooting over large parts of the Cerrado, in line with observations of deep rooting vegetation. While this method provides reasonably spatial variable maximum rooting depths, LPJmL-VR-SPITFIRE does not simulate an actual water table. In reality, deep-rooted trees can tap groundwater, but LPJmL-VR-SPITFIRE assumes free drainage, preventing this interaction. Consequently, some areas may experience artificially shallow rooting depths (e.g. Amazonian floodplains) without the benefit of accessing deeper water

704 reserves, a factor that could become important, especially when running future simulations
705 with the model. Considering these aspects in future work, especially global studies, could
706 further improve the representation of belowground competition and resulting spatial
707 vegetation distribution.

708

709 5. Conclusion

710 The parameterization of the new Tropical Broadleaved Savanna PFT (TrBS) in LPJmL-
711 VR-SPITFIRE significantly improves the representation of the Cerrado biome, the second-
712 largest vegetation formation in South America, in terms of belowground vs aboveground
713 competition, vegetation dynamics and fire. By inclusion of variable rooting strategies
714 along with recent process-based fire modeling, and a new drought mortality function, we
715 present a model that is suited to study complex ecological interactions of the sensitive
716 Cerrado biome that are rapidly changing under ongoing climate change. Here, we
717 combined literature and observational data to parameterize the TrBS PFT and to adjust
718 parameters of tree and root allocation functions, among others. Introducing a dedicated
719 vegetation type for tropical savannas and combining with variable rooting strategies will
720 equip DGVMs to make more precise assessments of recovery, reforestation, and
721 regeneration strategies in these unique ecosystems. By refining the modeling of savanna
722 dynamics, this study provides a valuable foundation for improving conservation strategies,
723 land-use planning, and climate mitigation efforts in fire-prone landscapes such as the
724 Cerrado. The introduction of a savanna-specific PFT with deeper rooting depth not only
725 led to a more realistic allocation of carbon belowground but also enabled the model to
726 reproduce the iconic “upside-down forest” structure of the Cerrado. This structural realism
727 also translated into better representation of vegetation distribution, fire regimes, and their
728 seasonal patterns. These results underscore the importance of incorporating trait diversity,

729 particularly rooting strategies, into DGVMs. Building on this progress, future work, such
730 as extending this savanna-specific PFT to individual-based models like LPJmL-FIT, can
731 further enhance our understanding of post-fire recovery dynamics interacting with
732 functional diversity and more clearly distinguish the intrinsic ecological behavior of
733 tropical savannas from that of tropical forests.

734

735 **6. Code and Data Availability**

736 The LPJmL-VR-SPITFIRE model is open-source and available at
737 [\[10.5281/zenodo.16965740\]](https://doi.org/10.5281/zenodo.16965740). Field survey data used in this study are available from the
738 corresponding author upon reasonable request. All other relevant data supporting the
739 findings of this study are available from the authors or included in the supplementary
740 materials.

741

742 **7. Competing interests**

743 One author is a member of the editorial board of journal "Biogeosciences".

744

745 **8. Author contributions**

746 *J.S.: Data curation, Formal analysis, Visualization, Writing – original draft

747 *S.B.: Methodology and Software, Formal analysis, Visualization, Writing – original
748 draft

749 W.v.B.: Methodology and Software, Writing – review and editing

750 M.Bi.: Methodology and Software, Writing – review and editing

751 B.S.: Conceptualization, Writing – review and editing

752 L.O.: Writing – review and editing

753 K.Th.: Supervision, Writing – review and editing

754 M.Bu.: Supervision, Writing – review and editing

755

756 **9. Acknowledgments**

757 The authors are grateful to PIK and the Graduate Program in Ecology from UnB for
758 providing the infrastructure and assistance without which this project wouldn't be possible.

759 To all researchers from the Ecosystems in Transition group at PIK and the Ecosystems
760 Ecology Lab at UnB that contributed with suggestions, critiques, points and ideas. Special
761 thanks to Letícia Gomes, Isabel Castro, Waira Machida, Lucas Costa and Felipe Lenti for
762 sharing their field data, essential for this work. Boris Sakschewski is part of the Planetary
763 Boundaries Science Lab.

764

765 **10. Funding Information**

766 J.S. acknowledges the funding by the National Coordination for High Level Education and
767 Training (CAPES) through the Internationalization Program (PrInt), grant number
768 88887.891863/2023-00. This work was supported by the National Institute of Science and
769 Technology for Climate Change Phase 2 under CNPq grant 465501/2014-1, FAPESP grant
770 2014/50848-9 and CAPES grant 88881.146050/2017-01. S.B. gratefully acknowledges
771 funding by the Conservation International Foundation, grant number CI-114129. This
772 project has received funding from the European Union's Horizon 2020 research and
773 innovation program under grant agreement No 101003890 (FirEURisk). The authors
774 gratefully acknowledge the Ministry of Research, Science and Culture (MWFK) of Land
775 Brandenburg for supporting this project by providing resources on the high-performance
776 computer system at the Potsdam Institute for Climate Impact Research.

777

778 **11. References**

779 Baudena, M., Dekker, S. C., Van Bodegom, P. M., Cuesta, B., Higgins, S. I., Lehsten, V.,
780 Reick, C. H., Rietkerk, M., Scheiter, S., Yin, Z., Zavala, M. A., and Brovkin, V.: Forests,
781 savannas, and grasslands: Bridging the knowledge gap between ecology and Dynamic
782 Global Vegetation Models, *Biogeosciences*, 12, 1833–1848, <https://doi.org/10.5194/bg-12-1833-2015>, 2015.

784 Bowman, D. M. J. S., Balch, J. K., Artaxo, P., Bond, W. J., Carlson, J. M., Cochrane, M.
785 A., D'Antonio, C. M., DeFries, R. S., Doyle, J. C., Harrison, S. P., Johnston, F. H.,
786 Keeley, J. E., Krawchuk, M. A., Kull, C. A., Marston, J. B., Moritz, M. A., Prentice, I.
787 C., Roos, C. I., Scott, A. C., ... Pyne, S. J: Fire in the Earth System, *Science*, 324, 481–
788 484, <https://doi.org/10.1126/science.1163886>, 2009.

789 Bustamante, M. M. C., Nardoto, G. B., Pinto, A. S., Resende, J. C. F., Takahashi, F. S. C.,
790 and Vieira, L. C. G.: Potential impacts of climate change on biogeochemical functioning
791 of Cerrado ecosystems. *Braz. J. Biol.*, 72, 655–671, <https://doi.org/10.1590/S1519-69842012000400005>, 2012.

793 Bustamante, M. M. C., Silva, J. S., Scariot, A., Sampaio, A. B., Mascia, D. L., Garcia, E.,
794 Sano, E., Fernandes, G. W., Durigan, G., Roitman, I., Figueiredo, I., Rodrigues, R. R.,
795 Pillar, V. D., de Oliveira, A. O., Malhado, A. C., Alencar, A., Vendramini, A., Padovezi,
796 A., Carrascosa, H., ... Nobre, C.: Ecological restoration as a strategy for mitigating and
797 adapting to climate change: Lessons and challenges from Brazil. *Mitig. Adapt. Strat. Gl.*,
798 24, 1249–1270, <https://doi.org/10.1007/s11027-018-9837-5>, 2019.

799 Bustamante, M., Medina, E., Asner, G., Nardoto, G., and Garcia-Montiel, D.: Nitrogen
800 cycling in tropical and temperate savannas, *Biogeochemistry*, 79, 209–237,
801 <https://doi.org/10.1007/s10533-006-9006-x>, 2006.

802 Cano-Crespo, A., Oliveira, P. J. C., Boit, A., Cardoso, M., and Thonicke, K.: Forest edge
803 burning in the Brazilian Amazon promoted by escaping fires from managed pastures, *J.
804 Geophys. Res-Biogeo.*, 120, 2095-2107, <https://doi.org/10.1002/2015JG002914>, 2015.

805 Carvalhais, N., Forkel, M., Khomik, M., Bellarby, J., Jung, M., Migliavacca, M., Mu, M.,
806 Saatchi, S., Santoro, M., Thurner, M., Weber, U., Ahrens, B., Beer, C., Cescatti, A.,

807 Randerson, J. T., and Reichstein, M.: Global covariation of carbon turnover times with
808 climate in terrestrial ecosystems, *Nature*, 51, 213–217,
809 <https://doi.org/10.1038/nature13731>, 2014.

810 Christian, H. J., Blakeslee, R. J., Boccippio, D. J., Boeck, W. L., Buechler, D. E., Driscoll,
811 K. T., Goodman, S. J., Hall, J. M., Koshak, W. J., Mach, D. M., and Stewart, M. F.:
812 Global frequency and distribution of lightning as observed from space by the Optical
813 Transient Detector, *J. Geophys. Res.-Atmos.*, 108, ACL 4-1-ACL 4-15,
814 <https://doi.org/10.1029/2002JD002347>, 2003.

815 Costa, L.: Nutrient enrichment changes water transport structures of savanna woody plants,
816 figshare, <https://doi.org/10.6084/m9.figshare.13252052.v1>, 2020.

817 Cramer, W., Bondeau, A., Woodward, F. I., Prentice, I. C., Betts, R. A., Brovkin, V., Cox,
818 P. M., Fisher, V., Foley, J. A., Friend, A. D., Kucharik, C., Lomas, M. R., Ramankutty,
819 N., Sitch, S., Smith, B., White, A., and Young-Molling, C.: Global response of terrestrial
820 ecosystem structure and function to CO₂ and climate change: Results from six dynamic
821 global vegetation models, *Glob. Change Biol.*, 7, 357–373,
822 <https://doi.org/10.1046/j.1365-2486.2001.00383.x>, 2001.

823 de Camargo, M. G. G., de Carvalho, G. H., Alberton, B. D. C., Reys, P., and Morellato, L.
824 P. C.: Leafing patterns and leaf exchange strategies of a cerrado woody community.
825 *Biotropica*, 50, 442–454. <https://doi.org/10.1111/btp.12552>, 2018.

826 D'Onofrio, D., Baudena, M., Lasslop, G., Nieradzik, L. P., Wårliind, D., and von
827 Hardenberg, J.: Linking vegetation-climate-fire relationships in Sub-Saharan Africa to
828 key ecological processes in two dynamic global vegetation models, *Fr. Environ. Sci.*, 8,
829 <https://doi.org/10.3389/fenvs.2020.00136>, 2020.

830 de Queiroz, L.P., Cardoso, D., Fernandes, M.F., Moro, M.F: Diversity and Evolution of
831 Flowering Plants of the Caatinga Domain., In: Silva, J.M.C., Leal, I.R., Tabarelli, M.
832 (eds) *Caatinga*. Springer-Cham, https://doi.org/10.1007/978-3-319-68339-3_2, 2017.

833 Drüke, M., Forkel, M., von Bloh, W., Sakschewski, B., Cardoso, M., Bustamante, M.,
834 Kurths, J., and Thonicke, K.: Improving the LPJmL4-SPITFIRE vegetation–fire model

835 for South America using satellite data, *Geosci. Model Dev.*, 12, 5029–5054,
836 <https://doi.org/10.5194/gmd-12-5029-2019>, 2019.

837 Feron, S., Cordero, R. R., Damiani, A., MacDonell, S., Pizarro, J., Goubanova, K.,
838 Valenzuela, R., Wang, C., Rester, L., and Beaulieu, A.: South America is becoming
839 warmer, drier, and more flammable. *Commun. Earth Environ.*, 5, 501,
840 <https://doi.org/10.1038/s43247-024-01654-7>, 2024.

841 Forkel, M., Carvalhais, N., Schaphoff, S., V. Bloh, W., Migliavacca, M., Thurner, M., and
842 Thonicke, K.: Identifying environmental controls on vegetation greenness phenology
843 through model–data integration. *Biogeosciences*, 11, 7025–7050.
844 <https://doi.org/10.5194/bg-11-7025-2014>, 2014.

845 Gomes, L., Miranda, H. S., and Bustamante, M. M. C.: How can we advance the knowledge
846 on the behavior and effects of fire in the Cerrado biome? *Forest Ecol. Manag.*, 417, 281–
847 290. <https://doi.org/10.1016/j.foreco.2018.02.032>, 2018.

848 Gomes, L., Miranda, H. S., Soares-Filho, B., Rodrigues, L., Oliveira, U., and Bustamante,
849 M. M. C.: Responses of plant biomass in the Brazilian savanna to frequent fires, *Front.*
850 *Forest Glob. Change*, 3, 507710. <https://doi.org/10.3389/ffgc.2020.507710>, 2020a.

851 Gomes, L., Miranda, H. S., Silvério, D. V., and Bustamante, M. M. C.: Effects and
852 behaviour of experimental fires in grasslands, savannas, and forests of the Brazilian
853 Cerrado, *Forest Ecol. Manag.* 458, 117804.
854 <https://doi.org/10.1016/j.foreco.2019.117804>, 2020b.

855 Gomes, L., Schüler, J., Silva, C., Alencar, A., Zimbres, B., Arruda, V., Silva, W. V. da,
856 Souza, E., Shimbo, J., Marimon, B. S., Lenza, E., Fagg, C. W., Miranda, S., Morandi, P.
857 S., Marimon-Junior, B. H., and Bustamante, M.: Impacts of fire frequency on net CO₂
858 emissions in the Cerrado savanna vegetation, *Fire*, 7, 208,
859 <https://doi.org/10.3390/fire7080280>, 2024.

860 Grimm, A. M., Vera, C. S., and Mechoso, C. R.: The South American monsoon system,
861 In: *The Global Monsoon System: Research and Forecast*, WMO/TD 1266, TMRP
862 Rep. 70, 219–238, Available at <https://core.ac.uk/download/pdf/36730348.pdf>, 2005.

863 Guglielmo, M., Tang, F. H. M., Pasut, C., and Maggi, F.: SOIL-WATERGRIDS,
864 mapping dynamic changes in soil moisture and depth of water table from 1970 to
865 2014, *Scient. Data*, 8, 263. <https://doi.org/10.1038/s41597-021-01032-4>, 2021.

866 Hengl, T., Walsh, M. G., Sanderman, J., Wheeler, I., Harrison, S. P., and Prentice, I. C.:
867 Global mapping of potential natural vegetation: An assessment of machine learning
868 algorithms for estimating land potential, *PeerJ*, 6, e5457,
869 <https://doi.org/10.7717/peerj.5457>, 2018.

870 Hersbach, H., Bell, B., Berrisford, P., Hirahara, S., Horányi, A., Muñoz-Sabater,
871 J., Nicolas, J., Peubey, C., Radu, R., Schepers, D., Simmons, A., Soci, C., Abdalla, S.,
872 Abellán, X., Balsamo, G., Bechtold, P., Biavati, G., Bidlot, J., Bonavita, M., ...
873 Thépaut, J. N. (2020). The ERA5 global reanalysis. *Quarterly Journal of the Royal
874 Meteorological Society*, 146, 1999–2049. <https://doi.org/10.1002/qj.3803>

875 Hoffmann, W. A., Adasme, R., Haridasan, M., T. De Carvalho, M., Geiger, E. L., Pereira,
876 M. A. B., Gotsch, S. G., and Franco, A. C.: Tree topkill, not mortality, governs the
877 dynamics of savanna–forest boundaries under frequent fire in central Brazil, *Ecology*,
878 90, 1326–1337, <https://doi.org/10.1890/08-0741.1>, 2009.

879 Hoffmann, W. A., da Silva, E. R., Machado, G. C., Bucci, S. J., Scholz, F. G., Goldstein,
880 G., and Meinzer, F. C.: Seasonal leaf dynamics across a tree density gradient in a
881 Brazilian savanna, *Oecologia*, 145, 306–315, <https://doi.org/10.1007/s00442-005-0129-x>, 2005.

883 Hoffmann, W. A., Orthen, B., and Franco, A. C.: Constraints to seedling success of savanna
884 and forest trees across the savanna-forest boundary, *Oecologia*, 140, 252–260,
885 <https://doi.org/10.1007/s00442-004-1595-2>, 2004.

886 Hofmann, G., Cardoso, M., Alves, R., Weber, E., Barbosa, A., De Toledo, P., Pontual, F.,
887 Salles, L., Hasenack, H., Passos Cordeiro, J. L., Aquino, F., and Oliveira, L.: The
888 Brazilian Cerrado is becoming hotter and drier, *Glob. Change Biol.*, 27,
889 <https://doi.org/10.1111/gcb.15712>, 2021.

890 IBGE: Brazilian Vegetation, Available at
891 <https://www.ibge.gov.br/en/geosciences/maps/state-maps/19470-brazilian-vegetation.html?andt=downloads>, 2017.

893 IBGE: Biomas e Sistema Costeiro-Marinho do Brasil—PGI, Available at
894 <https://www.ibge.gov.br/apps/biomas/#/home>, 2024.

895 Jackson, R. B., Canadell, J., Ehleringer, J. R., Mooney, H. A., Sala, O. E., and Schulze, E.
896 D.: A global analysis of root distributions for terrestrial biomes, *Oecologia*, 108, 389–
897 411. <https://doi.org/10.1007/BF00333714>, 1996.

898 Klein Goldewijk, K., Beusen, A., Drecht, G., and Vos, M.: The HYDE 3.1 spatially explicit
899 database of human-induced global land-use change over the past 12,000 years, *Global*
900 *Ecol Biogeogr.*, 20, 73–86, <https://doi.org/10.1111/j.1466-8238.2010.00587.x>, 2011.

901 Langan, L., Higgins, S. I., and Scheiter, S.: Climate-biomes, pedo-biomes or pyro-biomes:
902 which world view explains the tropical forest–savanna boundary in South America? *J.*
903 *Biogeogr.*, 44, 2319–2330, <https://doi.org/10.1111/jbi.13018>, 2017.

904 Lehmann, C. E. R., Anderson, T. M., Sankaran, M., Higgins, S. I., Archibald, S., Hoffmann,
905 W. A., Hanan, N. P., Williams, R. J., Fensham, R. J., Felfili, J., Hutley, L. B., Ratnam,
906 J., San Jose, J., Montes, R., Franklin, D., Russell-Smith, J., Ryan, C. M., Durigan, G.,
907 Hiernaux, P., ... Bond, W. J.: Savanna vegetation-fire-climate relationships differ among
908 continents. *Science*, 343, 548–552, <https://doi.org/10.1126/science.1247355>, 2014.

909 Machida, W. S., Gomes, L., Moser, P., Castro, I. B., Miranda, S. C., da Silva-Júnior, M.
910 C., and Bustamante, M. M. C.: Long term post-fire recovery of woody plants in
911 savannas of central Brazil, *Forest Ecol. Manag.*, 493, 119255.
912 <https://doi.org/10.1016/j.foreco.2021.119255>, 2021.

913 Malhi, Y., Aragão, L. E. O. C., Galbraith, D., Huntingford, C., Fisher, R., Zelazowski, P.,
914 Sitch, S., McSweeney, C., and Meir, P.: Exploring the likelihood and mechanism of a
915 climate-change-induced dieback of the Amazon rainforest, *P. Natl. A. Sci.*, 106, 20610–
916 20615, <https://doi.org/10.1073/pnas.0804619106>, 2009.

917 MapBiomass 9.0: MapBiomass Uso e Cobertura 9.0, Available at
918 <https://brasil.mapbiomas.org/colecoes-mapbiomas/>, 2024.

919 MapBiomas Fogo: MapBiomas Fogo 3.0, Available at
920 <https://mapbiomasfogocol3v1.netlify.app/index.html>, 2024.

921 MapBiomas Fogo: MapBiomas Fogo 4.0, Available at https://brasil.mapbiomas.org/wp-content/uploads/sites/4/2025/06/Fact_Fogo_colecao4.pdf, 2025.

922
923 Martens, C., Hickler, T., Davis-Reddy, C., Engelbrecht, F., Higgins, S. I., Von Maltitz, G.
924 P., Midgley, G. F., Pfeiffer, M., and Scheiter, S.: Large uncertainties in future biome
925 changes in Africa call for flexible climate adaptation strategies, *Glob. Change Biol.*, 27,
926 340–358 <https://doi.org/10.1111/gcb.15390>, 2021.

927 MCTI: Quarto inventário nacional de emissões e remoções antrópicas de gases de efeito
928 estufa setor uso da terra, mudança do uso da terra e florestas, Available at:
929 <https://repositorio.mcti.gov.br/handle/mctic/4782>, 2020.

930 MCTI: First biennial transparency report of Brazil to the United Nations Framework
931 Convention on Climate Change, Available at: <https://www.gov.br/mcti/pt-br/accompanhe-o-mcti/sirene/publicacoes/relatorios-bienais-de-transparencia-btrs>, 2024.

932
933 Moncrieff, G. R., Scheiter, S., Langan, L., Trabucco, A., and Higgins, S. I.: The future
934 distribution of the savannah biome: model-based and biogeographic contingency, *Philos.
935 T. R. Soc. B.*, 371, 20150311, <https://doi.org/10.1098/rstb.2015.0311>, 2016.

936 Myers, N., Mittermeier, R. A., Mittermeier, C. G., da Fonseca, G. A. B., and Kent, J.:
937 Biodiversity hotspots for conservation priorities, *Nature*, 403, 853–858.
938 <https://doi.org/10.1038/35002501>, 2000.

939 Oberhagemann, L., Billing, M., Von Bloh, W., Drüke, M., Forrest, M., Bowring, S. P. K.,
940 Hetzer, J., Ribalaygua Batalla, J., and Thonicke, K.: Sources of uncertainty in the global
941 fire model SPITFIRE: development of LPJmL-SPITFIRE1.9 and directions for future
942 improvements, *Geosci. Model Dev.*, 18, 2021–2025, <https://doi.org/10.5194/gmd-18-2021-2025>, 2025.

943
944 Oliveira, R. S., Bezerra, L., Davidson, E. A., Pinto, F., Klink, C. A., Nepstad, D. C., and
945 Moreira, A.: Deep root function in soil water dynamics in cerrado savannas of central
946 Brazil. *Funct. Ecol.*, 19, 574–581, <https://doi.org/10.1111/j.1365-2435.2005.01003.x>,
947 2005.

948 Oliveira, U., Soares-Filho, B., de Souza Costa, W. L., Gomes, L., Bustamante, M., and
949 Miranda, H.: Modeling fuel loads dynamics and fire spread probability in the Brazilian
950 Cerrado, Forest Ecol. Manag., 482, 118889,
951 <https://doi.org/10.1016/j.foreco.2020.118889>, 2021.

952 Oliver, T. H., Heard, M. S., Isaac, N. J. B., Roy, D. B., Procter, D., Eigenbrod, F.,
953 Freckleton, R., Hector, A., Orme, C. D. L., Petchey, O. L., Proença, V., Raffaelli, D.,
954 Suttle, K. B., Mace, G. M., Martín-López, B., Woodcock, B. A., and Bullock, J. M.:
955 Biodiversity and resilience of ecosystem functions. Trends Ecol. Evol., 30, 673–684,
956 <https://doi.org/10.1016/j.tree.2015.08.009>, 2015.

957 Peel, M. C., Finlayson, B. L., and McMahon, T. A.: Updated world map of the Köppen-
958 Geiger climate classification, Hydrol. Earth Syst. Sc., 11, 1633–1644,
959 <https://doi.org/10.5194/hess-11-1633-2007>, 2007.

960 Perkins, O., Kasoar, M., Voulgarakis, A., Smith, C., Mistry, J., and Millington, J. D. A.
961 (2024). A global behavioural model of human fire use and management: WHAM! v1.0,
962 Geosci. Model Dev., 17, 3993–4016, <https://doi.org/10.5194/gmd-17-3993-2024>, 2024.

963 Pivello, V. R.: The Use of fire in the Cerrado and amazonian rainforests of Brazil: past and
964 present. Fire Ecol., 7, 24-39. <https://doi.org/10.4996/fireecology.0701024>, 2011.

965 Ratnam, J., Bond, W. J., Fensham, R. J., Hoffmann, W. A., Archibald, S., Lehmann, C. E.
966 R., Anderson, M. T., Higgins, S. I., and Sankaran, M.: When is a ‘forest’ a savanna, and
967 why does it matter? Global Ecol. Biogeogr., 20, 653–660. <https://doi.org/10.1111/j.1466-8238.2010.00634.x>, 2011.

969 Ribeiro, J., and Walter, B.: As principais fitofisionomias do bioma Cerrado In: Sano, S.M.,
970 Almeida, S.P. and Ribeiro, J.F. (Eds.), Cerrado Ecologia e Flora, p. 152–212., 2008.

971 Rodrigues, A. A., Macedo, M. N., Silvério, D. V., Maracahipes, L., Coe, M. T., Brando, P.
972 M., Shimbo, J. Z., Rajão, R., Soares-Filho, B., and Bustamante, M. M. C.: Cerrado
973 deforestation threatens regional climate and water availability for agriculture and
974 ecosystems, Glob. Change Biol., 28, 6807–6822, <https://doi.org/10.1111/gcb.16386>,
975 2022.

976 Ronquim, C. C., Prado, C. H. B. de A., and de Paula, N. F.: Growth and photosynthetic
977 capacity in two woody species of cerrado vegetation under different radiation
978 availability, *Braz. Arch. Biol. Techn.*, 46, 243–252, <https://doi.org/10.1590/S1516-89132003000200016>, 2003.

980 Saboya, P., and Borghetti, F.: Germination, initial growth, and biomass allocation in three
981 native Cerrado species, *Braz. J. Bot.*, 35, 129–135, <https://doi.org/10.1590/S0100-84042012000200002>, 2012.

983 Sakschewski, B., Von Bloh, W., Boit, A., Rammig, A., Kattge, J., Poorter, L., Peñuelas, J.,
984 and Thonicke, K.: Leaf and stem economics spectra drive diversity of functional plant
985 traits in a dynamic global vegetation model, *Glob. Change Biol.*, 21, 2711–2725,
986 <https://doi.org/10.1111/gcb.12870>, 2015.

987 Sakschewski, B., von Bloh, W., Drüke, M., Sörensson, A. A., Ruscica, R., Langerwisch, F.,
988 Billing, M., Bereswill, S., Hirota, M., Oliveira, R. S., Heinke, J., and Thonicke, K.:
989 Variable tree rooting strategies are key for modelling the distribution, productivity and
990 evapotranspiration of tropical evergreen forests. *Biogeosciences*, 18, 4091–4116,
991 <https://doi.org/10.5194/bg-18-4091-2021>, 2021.

992 Salazar, A., Katzfey, J., Thatcher, M., Syktus, J., Wong, K., and McAlpine, C.:
993 Deforestation changes land–atmosphere interactions across South American biomes,
994 *Global Planet. Change*, 139, 97–108, <https://doi.org/10.1016/j.gloplacha.2016.01.004>,
995 2016.

996 Sano, E. E., Rodrigues, A. A., Martins, E. S., Bettoli, G. M., Bustamante, M. M. C., Bezerra,
997 A. S., Couto, A. F., Vasconcelos, V., Schüler, J., and Bolfe, E. L.: Cerrado ecoregions:
998 A spatial framework to assess and prioritize Brazilian savanna environmental diversity
999 for conservation, *J. Environ. Manage.*, 232, 818–828,
1000 <https://doi.org/10.1016/j.jenvman.2018.11.108>, 2019.

1001 Schaphoff, S., Von Bloh, W., Rammig, A., Thonicke, K., Biemans, H., Forkel, M., Gerten,
1002 D., Heinke, J., Jägermeyr, J., Knauer, J., Langerwisch, F., Lucht, W., Müller, C.,
1003 Rolinski, S., and Waha, K.: LPJmL4 – a dynamic global vegetation model with managed
1004 land – Part 1: Model description. *Geosci. Model Dev.*, 11, 1343–1375,
1005 <https://doi.org/10.5194/gmd-11-1343-2018>, 2018.

1006 Scholz, F. G., Bucci, S. J., Goldstein, G., Meinzer, F. C., Franco, A. C., and Salazar, A.:
1007 Plant- and stand-level variation in biophysical and physiological traits along tree density
1008 gradients in the Cerrado, *Braz. J. Plant Physiol.*, 20, 217–232,
1009 <https://doi.org/10.1590/S1677-04202008000300006>, 2008.

1010 Schüler, J.: Áreas prioritárias para a restauração no Cerrado: aumentando os benefícios e
1011 reduzindo os conflitos, Masters dissertation, Universidade de Brasília, 105 p. Available
1012 at <http://repositorio.unb.br/handle/10482/39518>, 2020.

1013 Schüler, J., and Bustamante, M. M. C.: Spatial planning for restoration in Cerrado:
1014 Balancing the trade-offs between conservation and agriculture, *J. Appl. Ecol.*, 59, 2616–
1015 2626, <https://doi.org/10.1111/1365-2664.14262>, 2022.

1016 Schumacher, V., Setzer, A., Saba, M. M. F., Naccarato, K. P., Mattos, E., and Justino, F.:
1017 Characteristics of lightning-caused wildfires in central Brazil in relation to cloud-ground
1018 and dry lightning. *Agr. Forest Meteorol.*, 312, 108723,
1019 <https://doi.org/10.1016/j.agrformet.2021.108723>, 2022.

1020 Shinozaki, K., Yoda, K., Hozumi, K., and Kira, T.: A quantitative analysis of plant form-
1021 the Pipe Model Theory: II. Further evidence of the theory and its application in forest
1022 ecology. *Jpn. J. Ecol.*, 14, 133–139. https://doi.org/10.18960/seitai.14.4_133, 1964.

1023 Simon, M. F., and Pennington, T.: Evidence for adaptation to fire regimes in the tropical
1024 savannas of the Brazilian Cerrado, *Int. J. Plant Sci.*, 173, 711–723,
1025 <https://doi.org/10.1086/665973>, 2012.

1026 Solbrig, O. T., Medina, E., and Silva, J. F.: Biodiversity and savanna ecosystem processes:
1027 A global perspective (Vol. 121). Springer, 1996.

1028 Souchie, F. F., Pinto, J. R. R., Lenza, E., Gomes, L., Maracahipes-Santos, L., and Silvério,
1029 D. V.: Post-fire resprouting strategies of woody vegetation in the Brazilian savanna, *Acta
1030 Bot. Bras.*, 31, 260–266, <https://doi.org/10.1590/0102-33062016abb0376>, 2017.

1031 Souza, C. R. D., Coelho De Souza, F., Françoso, R. D., Maia, V. A., Pinto, J. R. R., Higuchi,
1032 P., Silva, A. C., Prado Júnior, J. A. D., Farrapo, C. L., Lenza, E., Mews, H., Rocha, H.
1033 L. L., Mota, S. L., Rodrigues, A. L. C., Silva-Sene, A. M. D., Moura, D. M., Araújo, F.
1034 D. C., Oliveira, F. D., Gianasi, F. M., ... Santos, R. M. D.: Functional and structural

1035 attributes of Brazilian tropical and subtropical forests and savannas, *Forest Ecol. Manag.*,
1036 558, 121811, <https://doi.org/10.1016/j.foreco.2024.121811>, 2024.

1037 Strassburg, B. B. N., Brooks, T., Feltran-Barbieri, R., Iribarrem, A., Crouzeilles, R., Loyola,
1038 R., Latawiec, A. E., Oliveira Filho, F. J. B., Scaramuzza, C. A. de M., Scarano, F. R.,
1039 Soares-Filho, B., and Balmford, A.: Moment of truth for the Cerrado hotspot, *Nat. Ecol.
1040 Evol.*, 1, 1–3, <https://doi.org/10.1038/s41559-017-0099>, 2017.

1041 Swann, A. L. S., Longo, M., Knox, R. G., Lee, E., and Moorcroft, P. R.: Future deforestation
1042 in the Amazon and consequences for South American climate, *Agr. Forest Meteorol.*,
1043 214–215, 12–24, <https://doi.org/10.1016/j.agrformet.2015.07.006>, 2015.

1044 Syktus, J. I., and McAlpine, C. A.: More than carbon sequestration: Biophysical climate
1045 benefits of restored savanna woodlands, *Sci. Rep.-UK*, 6, 29194,
1046 <https://doi.org/10.1038/srep29194>, 2016.

1047 Terra, M. C. N. S., Nunes, M. H., Souza, C. R., Ferreira, G. W. D., Prado-Junior, J. A. do,
1048 Rezende, V. L., Maciel, R., Mantovani, V., Rodrigues, A., Morais, V. A., Scolforo, J. R.
1049 S., and Mello, J. M.: The inverted forest: Aboveground and notably large belowground
1050 carbon stocks and their drivers in Brazilian savannas, *Sci. Total Environ.*, 867, 161320,
1051 <https://doi.org/10.1016/j.scitotenv.2022.161320>, 2023.

1052 Terra, M. D. C. N. S., Santos, R. M. D., Prado Júnior, J. A. D., De Mello, J. M., Scolforo,
1053 J. R. S., Fontes, M. A. L., Schiavini, I., Dos Reis, A. A., Bueno, I. T., Magnago, L. F. S.,
1054 and Ter Steege, H.: Water availability drives gradients of tree diversity, structure and
1055 functional traits in the Atlantic–Cerrado–Caatinga transition, Brazil, *J. Plant Ecol.*, 11,
1056 803–814, <https://doi.org/10.1093/jpe/fty017>, 2018.

1057 Thonicke, K., Billing, M., von Bloh, W., Sakschewski, B., Niinemets, Ü., Peñuelas, J.,
1058 Cornelissen, J. H. C., Onoda, Y., van Bodegom, P., Schaeppman, M. E., Schneider, F. D.,
1059 and Walz, A.: Simulating functional diversity of European natural forests along climatic
1060 gradients, *J Biogeogr.*, 47, 1069–1085, <https://doi.org/10.1111/jbi.13809>, 2020.

1061 Thonicke, K., Spessa, A., Prentice, I. C., Harrison, S. P., Dong, L., and Carmona-Moreno,
1062 C.: The influence of vegetation, fire spread and fire behavior on biomass burning and

1063 trace gas emissions: Results from a process-based model, *Biogeosciences*, 7, 1991–2011,
1064 <https://doi.org/10.5194/bg-7-1991-2010>, 2010.

1065 Tumber-Dávila, S. J., Schenk, H. J., Du, E., and Jackson, R. B.: Plant sizes and shapes above
1066 and belowground and their interactions with climate, *New Phytol.*, 235, 1032–1056,
1067 <https://doi.org/10.1111/nph.18031>, 2022.

1068 van der Werf, G. R., Randerson, J. T., Giglio, L., van Leeuwen, T. T., Chen, Y., Rogers, B.
1069 M., Mu, M., van Marle, M. J. E., Morton, D. C., Collatz, G. J., Yokelson, R. J., and
1070 Kasibhatla, P. S.: Global fire emissions estimates during 1997–2016, *Earth Syst. Sci.
1071 Data*, 9, 697–720, <https://doi.org/10.5194/essd-9-697-2017>, 2017.

1072 Von Bloh, W., Schaphoff, S., Müller, C., Rolinski, S., Waha, K., and Zaehle, S.:
1073 Implementing the nitrogen cycle into the dynamic global vegetation, hydrology, and crop
1074 growth model LPJmL (version 5.0), *Geosci. Model Dev.*, 11, 2789–2812,
1075 <https://doi.org/10.5194/gmd-11-2789-2018>, 2018.

1076 Whitley, R., Beringer, J., Hutley, L. B., Abramowitz, G., De Kauwe, M. G., Evans, B.,
1077 Haverd, V., Li, L., Moore, C., Ryu, Y., Scheiter, S., Schymanski, S. J., Smith, B., Wang,
1078 Y.-P., Williams, M., and Yu, Q.: Challenges and opportunities in land surface modelling
1079 of savanna ecosystems, *Biogeosciences*, 14, 4711–4732, <https://doi.org/10.5194/bg-14-4711-2017>, 2017.

1081 Wirth, S. B., Braun, J., Heinke, J., Ostberg, S., Rolinski, S., Schaphoff, S., Stenzel, F., von
1082 Bloh, W., Taube, F., and Müller, C.: Biological nitrogen fixation of natural and
1083 agricultural vegetation simulated with LPJmL 5.7.9, *Geosci. Model Dev.*, 17, 7889–
1084 7914, <https://doi.org/10.5194/gmd-17-7889-2024>, 2024.

1085 Wullschleger, S. D., Epstein, H. E., Box, E. O., Euskirchen, E. S., Goswami, S., Iversen, C.
1086 M., Kattge, J., Norby, R. J., van Bodegom, P. M., and Xu, X.: Plant functional types in
1087 Earth system models: Past experiences and future directions for application of dynamic
1088 vegetation models in high-latitude ecosystems, *Ann. Bot-London*, 114, 1–16.
1089 <https://doi.org/10.1093/aob/mcu077>, 2014.

1090 Zemp, D. C., Schleussner, C.-F., Barbosa, H. M. J., Hirota, M., Montade, V., Sampaio, G.,
1091 Staal, A., Wang-Erlandsson, L., and Rammig, A.: Self-amplified Amazon forest loss due

1092 to vegetation-atmosphere feedbacks, *Nature Commun.*, 8, 14681,
1093 <https://doi.org/10.1038/ncomms14681>, 2017.